Quaternary Research (2018), **89**, 201–222.

doi:10.1017/qua.2017.101

Calibrated density profiles of Caribbean mangrove peat sequences from computed tomography for assessment of peat preservation, compaction, and impacts on sea-level reconstructions

Marguerite A. Toscano[a]*, Juan L. Gonzalez[b], Kevin R.T. Whelan[c]

[a]Smithsonian Environmental Research Center, 647 Contees Wharf Road, Edgewater, Maryland 21037, USA
[b]School of Earth, Environmental and Marine Sciences, The University of Texas Rio Grande Valley, 1201 W. University Drive, Edinburg, Texas 78539, USA
[c]National Park Service, South Florida/Caribbean Inventory and Monitoring Network, 18001 Old Cutler Road, Suite 419, Miami, Florida 33157, USA

(Received May 23, 2017; Accepted October 30, 2017)

Abstract

Oceanic mangroves accumulate peat with sea-level rise without terrestrial sediment inputs, but fossil peat's elevation as a tide-range limited sea-level indicator is assumed to be affected by compaction. Despite assumption of decomposition, compression, and dewatering, pure *Rhizophora mangle* peat appears coarse, water-saturated, and loose even at depth. Calibrated peat densities from computed tomography (CT) and petrologic analysis allow quantitative assessment of compaction in continuous peats from Florida (6 m thick), Belize (12 m thick), and Panama (3.5 m thick). Pure peat exhibits voids at all depths and >80% water contents. CT density does not increase with depth; bulk densities are low, minimally variable, and trend-free. Higher CT-density intervals coincide with compositional changes (sediment, coral). CT of peat buried under sediment shows a shift to higher densities. CT of air-dried continuous peat shows uncompressed fine and coarse roots and voids, with negative densities indicative of air in place of interstitial water. Peat's high water content and hydraulic conductivity prevent dewatering and compaction, hypothetically maintaining original sea-level indicative elevations at intermediate depths. Non-compacted, sediment-free, offshore peats can provide a continuous proxy for reconstructing the record of sea-level rise at any site, if depositional, disturbance, and geochemical and biotic processes affecting ^{14}C ages are also assessed.

Keywords: Mangrove peat; Holocene sea-level proxy; Computed Tomography; Compaction; Hydraulic conductivity

INTRODUCTION

Reconstruction of Holocene sea-level rise (SLR) has been accomplished worldwide through geologic study and radiometric dating of leading-edge transgressive wetland deposits cored from a wide latitudinal and biological range of peat-forming estuarine, coastal, and open marine environments, tidal regimes, and sediment inputs. Accurate paleo sea-level reconstructions provide an essential linkage to modern tide gauge measurements (e.g., Gornitz, 1995; Donnelly et al., 2004; Gehrels and Woodworth, 2013). In the absence of, or correction for, tectonic overprints, paleo sea-level reconstructions have the potential to reveal rates of SLR with which peat-forming systems have kept pace in the recent geologic past as predictors of the sustainability of such systems into the next 50–100 yr under accelerating rates (Woodroffe, 1990; Ellison and Stoddart, 1991; Ellison, 1993; Parkinson et al., 1994; Field, 1995; Stumpf and Haines, 1998; NRC, 2005; Gehrels et al., 2005; Gilman et al., 2006; Church and White, 2006; Nicholls et al., 2007; Bindoff et al., 2007; Krauss et al., 2013).

Peat-based sea-level reconstruction relies in large part on obtaining accurate peat paleo elevations at the time of formation, i.e., sea level within the paleo tide range (Allen, 2000). Auto-compaction is a highly complex, ongoing, and long-term process that includes decay, compression, dewatering, and consolidation resulting in loss of void spaces and volume and reorientation of plant matter (Scholander et al., 1955; Kaye and Barghoorn, 1964; Skelton and Allaway, 1996; Allaway et al., 2001). It also increases bulk density as peat material is vertically displaced or pushed downward from its original depositional level through compression (Bird et al., 2004). Studies have suggested that it occurs during peat deposition, continues through time, and decreases asymptotically with depth (Kaye and Barghoorn, 1964; Pizzuto and Schwendt, 1997; Paul and Barras, 1998; Shaw and Ceman, 1999; Allen, 2000; Bird et al., 2004). These processes would effectively lower the elevation of

*Corresponding author at: Smithsonian Environmental Research Center, 647 Contees Wharf Road, Edgewater, Maryland 21037, USA. E-mail address: toscanom@si.edu (M.A. Toscano).

samples used to establish paleo-sea-level index points. While the potential influence of compaction on Holocene sea-level records is well recognized, it is commonly not quantified or modeled over millennial timescales because of the complexity involved to quantify its influence, yet arbitrary compaction corrections have been applied (e.g., Khan et al., 2015).

Compaction is assumed to affect all coastal peat types, from mainland salt marshes with meso- to macro-tidal ranges and significant siliciclastic sediment input (e.g., Williams, 2003), to open ocean mangrove islands in carbonate settings associated with coral reefs with microtidal ranges (e.g., Macintyre et al., 2004). The expectation of an ongoing process of compaction within Holocene peat deposits has governed/limited sea-level researchers' choice of samples for analysis to the extent that only basal peats sampled directly on pre-compacted or solid basement substrates are considered uncompacted and at their original depositional elevations. Thus, they have been regarded as the only reliable sea-level index points (e.g., Shennan et al., 2000; Törnqvist et al., 1998, 2008). The exclusive use of basal mangrove peats, particularly those resting on isolated buried carbonate banks, would severely limit the depth and age range of samples available to reconstruct Holocene SLR. In open-ocean settings dominated by organic matter with minimal or episodic sediment inputs, pure and thick mangrove peat sequences deposited above Pleistocene carbonate banks (e.g., Macintyre and Toscano, 2004) have been shown through ^{14}C dating to contain a record of the past 8 ka of Holocene SLR (e.g., Belize; Macintyre et al., 1995; Cameron and Palmer, 1995; Macintyre et al., 2004; McKee et al., 2007; Monacci et al., 2009). Macintyre et al. (2004) corrected for mechanical compaction from vibracoring, while McKee et al. (2007) and Monacci et al. (2009) used the non-compacting Russian peat borer, which introduces only minimal measurement- and non-vertical coring errors. However, auto-compaction due to peat decomposition and compression-induced compaction from overburden pressure may alter original depositional elevations so that even samples acquired with no mechanical compaction require the assumption of vertical displacement and increased error in elevation ranges.

In order to have greater confidence in the elevations of intermediate peats from continuous deposits as sea-level indicators, the challenge is to determine whether the thick peat sequences have been compacted/compressed, bioturbated, interrupted by mangrove diebacks, or otherwise disturbed. An objective, quantitative assessment of density and other attributes of the peat must be made to address the issues concerning expected and inherent elevation errors due to the presumption of peat compaction. The goal of this study is to investigate the evidence for compaction on mangrove peat over long sequences using imagery and quantitative density measurements from computed tomography (CT), an innovative method for assessing structure, texture, water, and sediment content/composition. This method derives high-resolution density profiles measured along the length of cored sequences, which help determine if peat sequences are progressively compacted and dewatered, which would result in increasing peat density with depth and time. Dried peat scanned from stored cores also reveals structural characteristics of peat, including fine root matrices, large root sections, and presence of void/air space, while peat cored from under ~4 m of sediment provides density metrics for a classic setting for compaction. CT data were integrated with standard peat petrologic analysis (dry bulk density, water content, and loss on ignition [LOI]) and to field (coring) observations of subsurface peat characteristics. To calibrate the CT density scale for oceanic peat deposits, allochthonous materials from surrounding lagoon and reef areas (sediments, carbonates, and drift seeds) that might be incorporated into the peat were scanned to aid in identification and comparison to peat densities. CT scans and petrology of peat buried under 3–5 m of siliciclastic sediments provide data from a setting conducive to compaction. We tested the hypothesis that thick, continuous, sediment-starved peat deposits are of consistent composition and density (i.e., not compacted) throughout. We propose that they provide more comprehensive and potentially continuous sea-level proxy records in sequences spanning the full elevation range of Holocene deposition than could be sampled over the local range of basal elevations. Determining the degree of peat compaction will also shed light on the subsurface hydrologic environment of open ocean peat sequences and the role of seawater saturation in maintaining paleo peat elevations over millennia of SLR.

PREVIOUS WORK

Toscano and Macintyre (2003) reconstructed Caribbean Holocene SLR as the western Atlantic sea level (WASL) curve, using the shallow reef crest coral *Acropora palmata* (Lighty et al., 1982) and intertidal *Rhizophora mangle* mangrove peat (Robbin, 1984; Digerfeldt and Hendry, 1989; Macintyre et al., 1995) as the main proxies for paleo sea levels. For their model, they assumed Holocene tectonic stability in the western Atlantic and Caribbean and microtidal ranges for all sites. The coral field exhibited elevations reflecting the habitat range (0– > 15 m; Lighty et al., 1982) of *A. palmata*, with the uppermost corals representing the reef crest, presumably within 1–2 m of sea level.

Intertidal *R. mangle* peat (composed overwhelmingly of fine surface and deeper-anchoring roots with lesser detrital components of leaf and wood fragments) forms essentially at the peat surface in the intertidal zone (e.g., Ono et al., 2006; McKee, 2011; Srikanth et al., 2016). Based on previous studies (e.g., Toscano and Macintyre, 2003; Macintyre et al., 2004; McKee et al., 2007), mangrove peat has the potential to be a precise sea-level indicator and act as an upper limit for sea-level models if age, elevation errors, and compaction can be accounted. The WASL curve included basal peats and peat sampled from intermediate levels in 7–10 m-thick sequences. Elevation errors due to mechanical compaction from vibracoring, push/piston coring and extrusion, and non-vertical coring were reduced where possible by field measurements (Macintyre et al., 1995, 2004). Control of core top elevations was minimized based on the small tidal and surface elevation ranges (Woodroffe, 1995; Kjerfve et al., 1982). Despite microtidal

https://doi.org/10.1017/qua.2017.101 Published online by Cambridge University Press

ranges, the peat field exhibited an elevation spread of up to 4 m above the coral field, as did a subset using only basal peats (Toscano and Macintyre, 2003), leading to lack of confidence in both ages and elevations of the peat data field to inform the placement of the WASL curve. Compaction is inconsistent with such a large positive elevation range in the data. Alternatively, up to 4 m tree heights cannot account for the high-plotting peats. Whole trees die, decay rapidly, are consumed by large cryptic insect populations (particularly termites) and disintegrate before they could be buried whole (assuming maximum measured peat accumulation of 0.4 cm/yr; McKee et al., 2007). Continuous peat sequences cored by us and presumably by other scholars (e.g., Macintyre et al., 1995, 2004; Wooller et al., 2007; McKee et al., 2007; McKee, 2011; Monacci et al., 2009) have not reported or dated standing canopy wood in the peat.

CT is a standard, non-destructive method for three-dimensional imaging and quantitative analysis of a wide range of organic and inorganic substances, including structural, compositional, and density measurements (Ketcham and Carlson, 2001; Cnudde and Boone, 2013). CT uses a narrowly collimated beam of X-rays that rotate around a sample and record images with a series of detectors positioned at various angles. As the sample moves through the X-ray beam, data are obtained as a series of vertical slices of <1 mm thickness. Quantitative imagery results from computer computation of X-ray absorption or attenuation to produce a representation of internal structure resulting from changes in attenuation or density. Reconstruction of the slices into a 3-dimensional unit allows for multi-dimensional views of the internal features of the sample. CT numbers, or Hounsfield Units (HU), are indicative of the amount of X-ray attenuation of elements or fabrics seen in the CT image and calibrated based on the attenuation produced by air (–1024 HU), the attenuation produced by water (0 HU), and the attenuation produced by bone (+1000 HU). Many other materials have been scanned in many scientific contexts. In the geosciences, CT has been applied to a number of complex analyses, such as to computing bulk densities in fine sediments (e.g., Amos et al., 1996); differentiating structures and components in peat and soil sciences (e.g., Pierret et al., 2002; Sleutel et al., 2008;Taina et al., 2008; Rezanezhad et al., 2009; Kettridge and Binley, 2011; Elyeznasni et al., 2012; Helliwell et al., 2013); measuring physical and hydraulic properties in peats (pore size, shape, distribution; Mooney, 2002; Quinton et al., 2009); identifying ice-rafted stones in deep sea sediment cores (e.g., Takana and Nakano, 2009); differentiating peat and sediment components of marsh soils (Davey et al., 2011); and determining 3-dimensional water distribution and soil macroporosity (Heijs et al., 1995).

METHODS

Field areas

We collected new continuous *R. mangle* peat cores spanning the Holocene history of sea-level changes at offshore mangrove islands along the upper Florida Keys, USA; the Mesoamerican Barrier Reef in Belize, Central America; and mangrove islands in the Bocas del Toro Archipelago, Panama. Our northern locality at Biscayne National Park, Florida contains an area of historically unaltered mangroves on the southeastern side of Swan Key (25°20.77'N, 80° 14.90'W, Fig. 1), consisting of 1 to > 6 m of continuous *R. mangle* peat sequences over the highly variable, high-relief surface of the late Pleistocene Key Largo Limestone (Stanley, 1966; Perkins, 1977; Multer et al., 2002). In Belize, the Twin Cays mangrove archipelago, (16°50.06'N, 88°06.4'W, Fig. 1) is constructed almost entirely of continuous mangrove peat deposits ranging in thickness from 7.5 to >12 m over Pleistocene carbonate bedrock (Macintyre et al., 1995; 2004; Macintyre and Toscano, 2004; McKee et al., 2007; Wooller et al., 2007). Our Panama sites (~9°14.93'N, 82°14.45'W, Fig. 1) have < 4 m of *R. mangle* peat in mangrove fringes surrounding siliciclastic islands (Coates et al., 2005). Sediment input to Panama mangrove peat is potentially a mixture of biogenic lagoonal carbonates and eroded siliceous sediments from the island interiors.

Additional calibration data include five basal Holocene peat samples from Morrosquillo, Colombia (9°33.87'N; 75° 32.88'W, Fig. 1), cored from beneath a 3–5-m-thick sedimentary unit, to provide an example of peats presumably compacted by overburden pressure (e.g., Bird et al., 2004). Lengths of air-dried peat cores from thick peat sequences in Belize (from Macintyre et al., 1995) were also scanned and analyzed to study the structural and density aspects of the peat in the absence of water saturation.

Coring methods and core site selection

We conducted reconnaissance auguring of mangrove sites to determine bedrock elevation ranges and continuity of peat sections, record horizons of interest, and examine the peat before taking pristine cores. We recorded subsurface peat characteristics, species, root density, woody intervals, wet and unrecoverable intervals, water content, allochthonous materials, and the presence and type of sediment. Cores were obtained using a Russian peat borer (RPB), which cuts peat from the side of the core hole in sequential 50 cm increments, eliminating mechanical compaction. Previously cored sites with known intermediate lagoonal carbonate lenses (Macintyre et al., 2004) were avoided. Only known/augured sites with continuous peat to bedrock were cored. Basal peat was attained when the RPB was stopped by pre-Holocene bedrock or impenetrable coral/carbonate sediment. The RPB has a 10 cm point to facilitate penetration, thus any basal sample was 10 cm above the actual bedrock level. The unsampled section between bedrock and lowest cored material may have contained marine carbonate sediment filling low areas of the platform prior to mangrove establishment or the true basal peat on bedrock, which we are unable to collect with this device. Compacted peats from Colombia were collected using a 6-cm-diameter gouge. Dried peat sections were vibracored (Macintyre et al., 1995).

https://doi.org/10.1017/qua.2017.101 Published online by Cambridge University Press

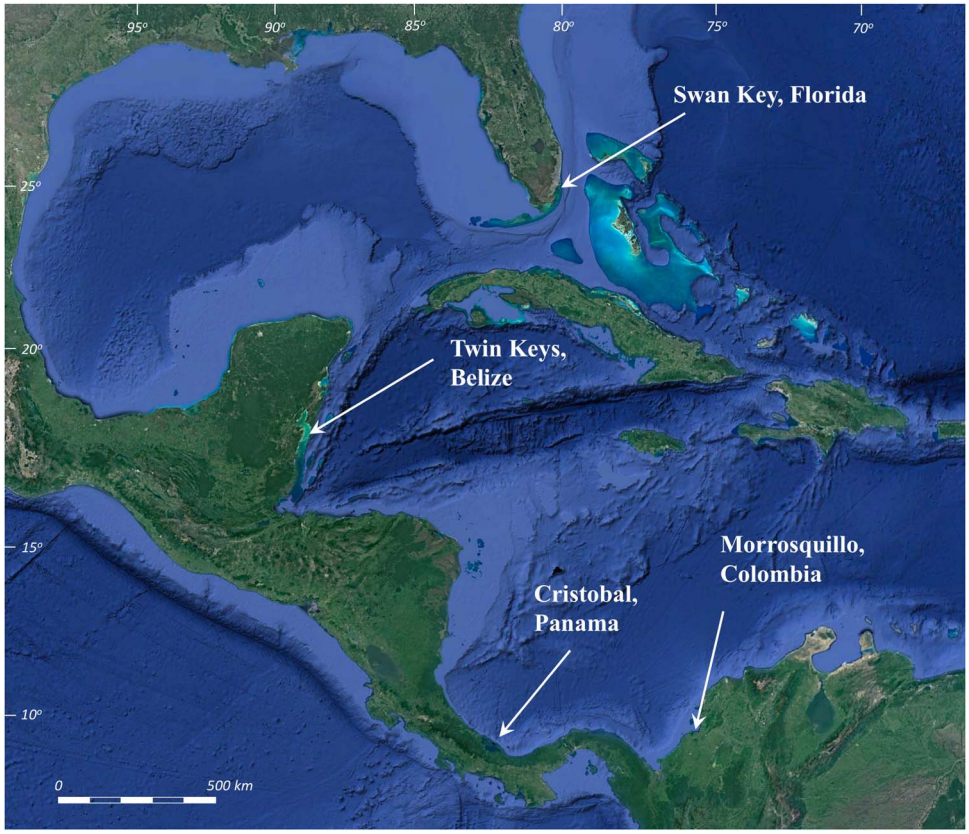

Figure 1. (color online) Mangrove core sites: Swan Key, Florida (25°20.77'N, 80°14.90'W); Twin Cays, Belize (16°50.06'N, 88° 06.4'W); Isla Cristobal, Panama (9°14.927'N, 82°14.455'W); and Morrosquillo, Colombia (9°33.87'N, 75°32.88'W).

Core processing

Peat core sections were visually examined and photographed upon collection and described by identifiable plant components and attributes of *R. mangle* at all sites plus *Avicennia germinans* in Belize. Identifications used diagnostic root structure and coloration, species-specific rhizomes, leaf fragments and wood, all of which aid paleoenvironmental interpretations (McKee and Vervaeke, 2010). Peat is visually and qualitatively described by the size and texture of plant remains, using the relative terms very coarse, coarse, finer, and pastier. Sand, identifiable coral fragments and hash (median particle size 2 mm to <64 mm; US Federal Geographic Data Committee, 2012) and carbonate mud are reported. Sections were thoroughly plastic-wrapped to prevent water loss, covered with plastic tubing, securely taped, and refrigerated. Whole cores were CT scanned at the Smithsonian Institution. Cores were also sampled at 10 cm intervals for bulk peat LOI analysis.

Computed tomography

We used standard CT methods, and calibrated densities of air, water and seawater, bone, and shallow coastal sediments (Amos et al., 1996; Davey et al., 2011) to provide a basic framework from which to evaluate the CT densities of scanned peats and incorporated sediments. Table 1 provides these published values with new reference densities in HUs determined for a range of potential local marine components (from environments adjacent to field sites) that may have been incorporated into peat over time (pumice pebbles, drift seeds, shell, and coral) to account for compositional changes. Table 1 includes HU averages for the compacted Colombian peats and the dried peat sections.

CT scanning of cores 6A (Swan Key, Biscayne, 6.5 m), 11A (Twin Cays, 11.66 m), single cores from two sites in Panama (Isla Cristobal, 3.5 m; Isla Popa, 3 m), compacted samples from Colombia, and dried peat, was completed using the Siemens Somatom Emotion Single Slice CT scanner at the National Museum of Natural History. Core sections were laid parallel to the long axis of the scanner bed and scanned in horizontal "slices" (Fig. 2A) at mA = 80 and KV = 130, with a slice width of 0.63 mm. Core scans were combined into a continuous series for each core section using a reconstruction increment of 0.6 mm, resulting in 823 slices over 493.8 mm, which accounted for 49.4 cm of the 49.6 cm core pipe length.

OsiriX was used to do initial density measurements on CT slices (Fig. 2A). Materialise Mimics Innovation Suite biomedical image processing software was used to create 3-d models of core contents. CT images of the peat textures were obtained from whole-core composition and using selected

https://doi.org/10.1017/qua.2017.101 Published online by Cambridge University Press

Table 1. HU densities for established calibrations (in bold) and new data for reef and mangrove-related materials collected in this study at field sites that might be encountered in CT scan data in peat cores. "CT slice" refers to a measurement taken from the surface of a 0.62 mm cross-sectional scan or "slice" of the material (Fig. 2A). "CT profile" represents a series of CT values or HUs at sub mm increments from a profile line along the core or sample. Dried peat is from Core TR7 from Macintyre et al. (1995; Belize). Compacted peat is from a deposit in Morrosquillo, Colombia.

Material scanned	Type	Mean HU	±2σ	Min.	Max.
Air	**Gas**	**–1024**			
Air[a]	**Gas**	**–994**	**9**		
Dried mangrove peat, CT slice	Plant matter	–567.24	152.98	–720.22	–414.26
Dried mangrove peat, CT slice	Plant matter	–506.86	141.31	–648.17	–365.55
Dried mangrove peat, CT slice	Plant matter	–583.23	185.86	–769.09	–397.37
Dried mangrove peat, CT slice	Plant matter	–661.82	169.15	–830.97	–492.67
Dried mangrove peat, CT slice	Plant matter	–570.54	169.29	–739.83	–401.25
Dried mangrove peat, TR7 CT profile 1	Plant matter; fine-coarse roots, wood, leaves	–681.84	251.98	–1024	432
Dried mangrove peat, TR7 CT profile 2	Plant matter; fine-coarse roots, wood, leaves	–672.5	221.84	–1024	238
Dried mangrove peat, TR7 CT profile 3	Plant matter; fine-coarse roots, wood, leaves	–709.67	222.58	–1024	206
Dried mangrove peat, TR7 CT profile 4	Plant matter; fine-coarse roots, wood, leaves	–703.29	228.72	–1024	303
Water	**Liquid**	**0**			
Fresh water[a]	**Liquid**	**6**	**11**		
Salt water[a]	**Liquid**	**54**	**11**		
Salt marsh (organic matter)[b]	**Coarse roots & rhizomes**	**–930–2**			
Salt marsh (organic matter)[b]	**Peat**	**13–264**			
Entada sp., CT slice	Drift seed (hard shell)	261.83	75.18	186.65	337.01
Mucuna sp., CT slice	Drift seed (hard shell)	213.05	20.47	192.58	233.47
Mucuna sp., CT slice	Drift seed (hard shell)	218.97	79.98	138.99	298.95
Fossil Coconut (in mangrove peat), CT slice	Drift seed (hard shell)	311.46	156.74	154.72	466.2
Fossil Coconut (in mangrove peat), CT slice	Drift seed (hard shell)	353.98	106.34	247.64	460.324
Compacted peat, CT profile	Dewatered peat and sediment	387.36	93.78	293.58	481.14
Compacted peat, CT profile	Dewatered peat and sediment	282.02	102.44	179.58	384.46
Particulates (clay, silt, mineral precipitates)[b]	**> 34% colloidal Silica; No sand-sized grains**	**265–750**			
Pumice (Rhyolitic), CT profile	> 70% SiO_2	464.96	111.7	353.26	576.66
Sand[b]	**Siliciclastic**	**751–1200**			
Bone	**Hydroxyapatites, collagen**	**1000**			
Core pipe	PVC	1420.161	23.2112	1242	1436
Oyster, CT slice	Shell	1776.73	1030.45	746.28	2807.18
Oyster, CT slice	Shell	2177.32	723.55	1453.77	2900.87
Acropora palmata, CT profile	Coral, caco3	3048.63	68.82	2979.81	3117.45
Acropora palmata, CT profile	Coral, caco3	3032.25	22.3	3009.95	3054.55
Acropora palmata, CT profile	Coral, caco3	3070.85	3.16	3067.69	3074.01
Rocks and Shells[b]	**General range**	**1201–3060**			
Plutonic Rock	Silicate minerals	3071			

[a]Measurements of Amos et al. (1996).
[b]Measurements of Davey et al. (2011) for sedimentary types.

density (HU) thresholds or ranges of interest to highlight specific components, such as peat matrix or sediment lenses (Fig. 2B–D). Profile lines were drawn along the long axis of each 3-d core image to obtain continuous quantitative density measurements in HUs.

Bulk Peat Analysis

We performed standard bulk peat and LOI analysis (at 550°C) to determine bulk density, water content, percentage of organics and inorganics, along with X-ray diffraction on ash samples to determine sediment mineralogy. Measured volumes of wet bulk peat were sampled at 10 cm intervals from Biscayne core 6A (50 samples/6.5 m core), Belize core 11A (107 samples/11.66 m core), a core from Isla Cristobal (33 samples/3.44 m core), a core from Isla Popa (29 samples/2.84 m core). The CT-scanned sample XII from Colombia is comparable in peat type and thickness of overburden to a separate sample from the same deposit, with 18 LOI samples at 10 cm spacing from –4.2 to –6.0 m relative to mean sea level (MSL). Dried peat, having no water, was not analyzed. Bulk samples were processed using standard procedures for LOI (Dean, 1974; Heiri et al., 2001; Chambers et al., 2011) and standard calculations to determine water content as

https://doi.org/10.1017/qua.2017.101 Published online by Cambridge University Press

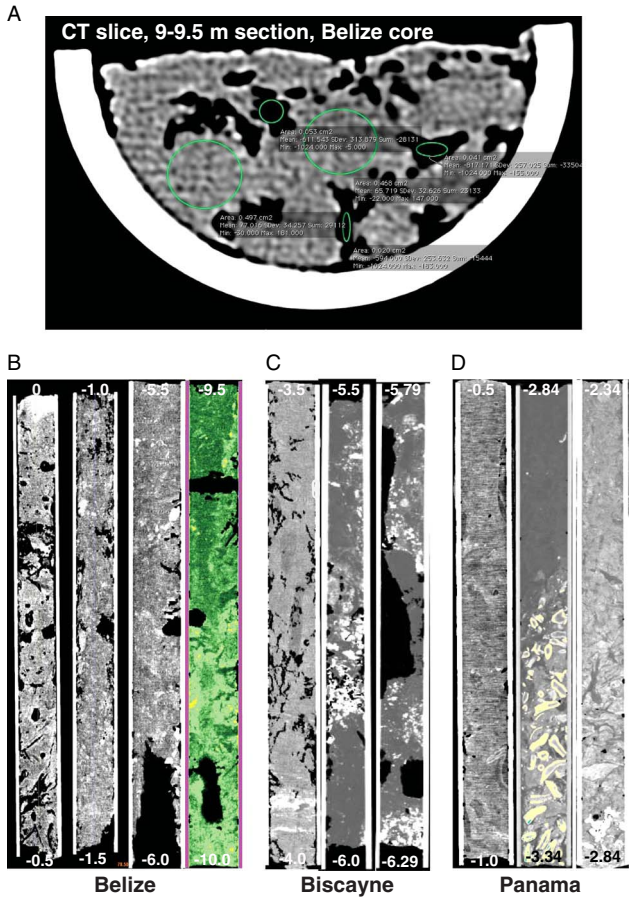

Figure 2. CT images of mangrove peat. (A) OsiriX image of CT slice from the 9–9.5 meter section of Belize core 11A. Green circles indicate locations of density measurements; density measurements indicated are not readable at this scale but values are given in Table 1. Black areas indicate voids. (B) CT topogram images of Belize core 11A sections 0–0.5 and 1.0–1.5 m; 5.5–6.0 m; 200 HU green mask in 9.5–10.0 m section. (C) Biscayne core sections 3.5–4.0 m showing high density sediment layer; overlapping sections covering 5.5–6.29 m with coral hash highlighted and watery voids. (D) Cristobal, Panama topograms showing typical peat from 0.5–1.0 m; carbonate material at base of Cristobal core highlighted by a 2500 HU yellow mask; and basal carbonate sediments in the Popa core. (For interpretation of the references to color in this figure legend, the reader is referred to the web version of this article.)

percent water by volume and mass, wet bulk density, dry bulk density, LOI, ash content, and ash-free (organic matter) bulk density.

X-Ray diffraction

Following LOI, mineralogic analysis by X-ray diffraction (XRD) was conducted on LOI_{550} ash residues of five Biscayne samples from a sediment-rich interval (400 to 450 cm) with visible coarse quartz grains in the 30 µm size range (some FeO-stained), carbonate and coral particles, low LOI, and high bulk density values. Nine ash samples from Panama cores (5 from Isla Cristobal and 4 from Isla Popa) covered the entire sample range from uppermost peat to sediment-rich basal sections. The Belize core contained no sediment, so ash was not analyzed.

Small (~100–150 mg) portions of ashed samples were ground in an alumina mortar and pestle in ethanol, then transferred to glass slides to dry. XRD scans were obtained on a Bruker D-80 system using Cu-Kα radiation, a range of 10–70° 2θ, and a scan speed of 2°/min. Bruker EVA software was used to do background subtraction and to identify the phases through the search/match program using the International Centre for Diffraction Data PDF-2 (2008) database (http://www.icdd.com/products/pdf2.htm). Phase abundances were estimated by comparing the most intense peaks for each mineral, adjusted by I/I_{cor} factors in the database. Intensity of the highest peak for each mineral divided by I/I_{cor} factor corrects for relative sensitivity.

RESULTS

Core analysis

We obtained continuous CT densities along complete peat sequences to determine the normal range of peat density and to look for evidence of increasing CT and dry bulk densities down core that might be indicative of compaction. We also looked for anomalous density values indicative of compositional changes in the core (sediment or allochthonous inputs, Table 1), and assessed CT densities in concert with bulk peat characteristics. XRD indicates that pure peat samples with CT densities close to that of seawater contain minor inorganic components such as marine salts (halite [NaCl], gypsum [$CaSO_4 \cdot 2H_2O$], anhydrite [$CaSO_4$], and thenardite [NaSO4]) related to seawater saturation of peat, and evaporation of higher salinity waters in mangrove pond environments. Aragonite ($CaCO_3$) is not detected by XRD in any peat-derived ash component despite obvious coral-rich basal sediment in several cores, which was not sampled for LOI. Calcite ($CaCO_3$) dominates (85%) the ash at 2.79 m (5 cm above the core base) in the Popa core, and at 3.29 m (the core base) of the Cristobal core (82%).

Florida

The deepest Biscayne peat core 6A at 6.29 m in length did not reach the high-relief surface of the underlying Pleistocene Key Largo Limestone on Swan Key; however, an adjacent core (6B; ~0.5 m away) reached bedrock at –4.5 m. Core 6A consisted of very coarse *R. mangle* peat from 0–3.0 m in core, coarse *R. mangle* peat to 4.0 m, somewhat finer/pastier peat with sediment to 4.5 m, followed by an extremely watery interval from 4.5–5.0 m that retrieved only small amounts of sand and peat. This was underlain by coarse/pasty wet *R. mangle* peat with stringy roots and quartz sand, underlain by coarse/pasty *R. mangle* peat to –6.29 m with *Diploria* sp. coral detritus. Although the core did not reach bedrock, it contains an interval with both sand and coral for contrast with peat CT density profiles (Fig. 3).

https://doi.org/10.1017/qua.2017.101 Published online by Cambridge University Press

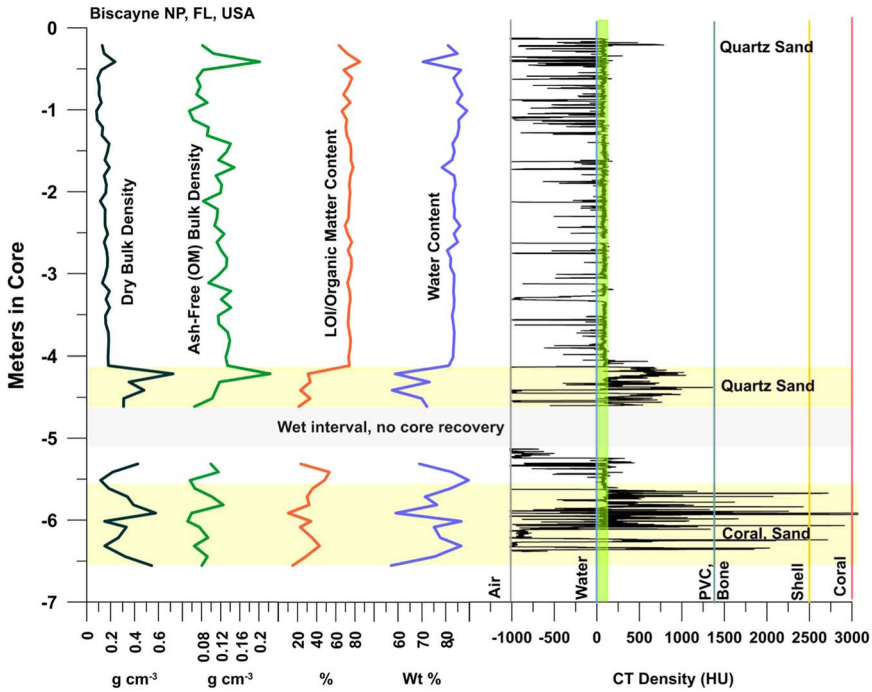

Figure 3. (color online) Graph of CT and bulk peat densities, LOI, and H_2O content for Biscayne Core 6A. See Figure 2C for selected topogram images. *R. mangle* peat forming the upper 4 m of core becomes mixed with siliciclastic sediment and carbonate material at ~–4 m. CT densities in the peat are consistently near the HU range for seawater (~60 HU). OMC ranges from 63–85% in the peat section. Bulk densities are approximately constant with no increasing trend with depth. Void (air) spaces occur at all depths as indicated by negative spikes in CT densities, even in the sediment intervals. Water contents are >80% in the peat, dropping to ~60% in sediment. Note un-cored interval (–4.5 to –5.0 m) due to excess water in the peat. Loose, wet peat also occurred at the base of the core at –6.29 m. Ash-free bulk densities determined for both the sediment-free peat (0.11 ± 0.03 g cm^{-3}) and lower section with sediment (0.09 ± 0.04 g cm^{-3}) are identical and show no trend suggesting increasing peat decomposition down core. Positive spikes occur at the top and in the –4 to –4.5 m section where sand was encountered.

CT/LOI /XRD

From 0–4.0 m in the core, pure *R. mangle* peat exhibits bulk densities from 0.082 to 0.237 g cm^{-3}, (mean 0.15 ± 0.33 g cm^{-3}; Fig. 3), which is consistent with tropical ombotrophic peats (Page et al., 2004) and other continuous offshore mangrove peat deposits (Monacci et al., 2009). LOI values representing organic matter content (OMC) are high, ranging from 63 to 85% in peat, but decreasing to 28.3 ± 5% in the lower sediment-rich interval. CT densities include negative numbers signifying void spaces, and peat values ranging from 24.2 to 104.1 HU. Ash yields from peat average 4.3%, from a minimum of 3.5% to a maximum of 7% at the top of the core where sand grains were observed. Water content of the peat interval (Table 2, Fig. 3) ranges from 70 to 89%, averaging 83%.

From 4.0–4.5 m, significant sediment present in the peat immediately increases bulk densities to a maximum of 0.72 g cm^{-3} (0.34 ± 0.16 g cm^{-3}) with order of magnitude higher ash yields to 36.7% (Table 2). Water content remains high, ranging from 57 to 89.6%, averaging 73%. Five samples had low (21–33%) LOI/OMC indicative of high inorganic matter values, generally high CT densities (238–769 HU; one void at –984 HU), coarse grains of quartz, and coral hash.

The interval from 4.5–5.0 m was too wet to recover a core, and from 5.0–5.5 m core recovery was low, again due to high subsurface water content (69–89%), but ash yields remain high due to sediment. CT values indicate voids at this level as well as typical values for peat (79 HU) and sandy peat (141.6 HU; Table 2, Fig. 3). From 5.5–6.29 m, water content (57–86%), ash (7.7–36.7%), and CT densities (66–1055; Table 2) remain high.

Ash-free bulk density ranges from 0.05 to 0.22 g cm^{-3}, which is similar to other peat types. Aside from anomalies at 0.3 and 4.1 m (Fig. 3) where quartz sand was also detected, virtually the same ash-free bulk densities were determined for both the sediment-free peat (0.11 ± 0.03 g cm^{-3}) and lower section with sediment (0.09 ± 0.04 g cm^{-3}). Ash samples analyzed via XRD were dominated by quartz (65–78%; Table 2) with small percentages of halite, anhydrite, and hematite. Despite coral hash seen in cores, no carbonates or gypsum were detected by XRD in the ash samples.

Belize

Core 11A consisted of 11.66 m of 100% *R. mangle* peat from top to Pleistocene bedrock; many similar thick, wet peat cores have been taken on Twin Cays. A basal carbonate sediment layer was not present above the RBP tip at this core site, and there was no discernable sediment throughout its length. The lowermost 50 cm of peat was extremely loose and wet and oozed from the coring device (Fig. 4).

https://doi.org/10.1017/qua.2017.101 Published online by Cambridge University Press

Table 2. Core description, CT densities, and LOI data for Biscayne Core 6A. *Rm* refers to *Rhizophora mangle* peat.

Biscayne Core 6A section (cm)	Core description	Depth in core (cm)	CT HU	Ash content weight (%)	Water content weight (%)	Dry bulk density (g cm^{-3})	LOI/ OMC	Ash-free (OM) bulk density (g cm^{-3})
0–50	Coarse, loose *Rm* peat, sandy at top	9.00	–278.98	6.991	80.961	0.129	0.633	0.082
		19.00	73.19	4.253	84.875	0.146	0.719	0.105
		29.00	102.51	4.340	70.429	0.237	0.851	0.202
		39.00	70.75	4.329	86.346	0.122	0.683	0.083
50–100	Very coarse *Rm* peat	49.00	71.56	3.870	83.282	0.092	0.769	0.070
		59.00	73.55	4.043	84.912	0.106	0.732	0.078
		69.00	70.59	4.203	86.845	0.102	0.680	0.070
		79.00	46.99	3.793	84.773	0.123	0.751	0.092
		89.00	53.23	3.729	88.927	0.082	0.663	0.054
100–150	Very coarse *Rm* peat	100.00	–275.59	4.161	85.402	0.088	0.715	0.063
		109.00	80.60	4.286	85.545	0.135	0.703	0.095
		119.00	84.07	4.3	84.900	0.128	0.715	0.092
		129.00	81.00	4.259	82.888	0.188	0.751	0.141
		139.00	86.64	3.912	83.633	0.174	0.761	0.132
		149.00	38.07	4.203	82.657	0.152	0.758	0.115
150–200	Very coarse *Rm* peat	158.00	–10.08	4.730	78.378	0.190	0.781	0.149
		168.00	78.74	4.063	83.556	0.146	0.753	0.110
		179.00	86.29	4.131	84.090	0.165	0.740	0.122
		189.00	83.99	4.198	83.207	0.160	0.750	0.120
		199.00	42.69	4.384	83.100	0.113	0.741	0.084
200–250	Very coarse *Rm* peat	209.00	79.26	4.280	83.772	0.154	0.736	0.114
		219.00	78.86	4.396	83.471	0.153	0.734	0.112
		229.00	53.53	4.244	85.995	0.154	0.697	0.107
		239.00	83.00	4.565	83.420	0.176	0.725	0.127
		249.00	–224.51	3.483	85.024	0.146	0.767	0.112
250–300	Very coarse *Rm* peat	259.00	24.18	5.289	80.623	0.166	0.727	0.121
		269.00	88.94	4.241	82.172	0.175	0.762	0.133
		279.00	97.53	4.263	81.927	0.173	0.764	0.132
		289.00	88.03	4.176	83.520	0.156	0.747	0.116
		299.00	–83.61	4.601	83.467	0.131	0.722	0.095
300–350	Coarse *Rm* peat	309.00	67.18	4.304	83.196	0.191	0.744	0.142
		319.00	–815.07	4.078	83.557	0.161	0.752	0.121
		329.00	93.46	4.333	83.401	0.192	0.739	0.142
		339.00	14.77	4.614	82.674	0.156	0.734	0.115
		349.00	86.30	4.588	83.207	0.160	0.727	0.116
350–400	Pastier, finer *Rm* peat	359.00	52.27	4.234	83.564	0.181	0.742	0.135
		369.00	90.40	4.043	83.448	0.184	0.756	0.139
		379.00	85.52	4.234	83.222	0.182	0.748	0.136
		389.00	90.23	4.514	83.071	0.178	0.733	0.131
		399.00	104.09	4.814	81.313	0.181	0.742	0.135
400–450	Watery, pastier *Rm* peat with quartz sand	409.00	768.61	28.421	58.838	0.722	0.310	0.223
	Sandy	419.00	311.78	17.923	73.140	0.354	0.333	0.118
	Voids	429.00	–983.68	32.694	57.554	0.479	0.230	0.110
	Sandy	439.00	237.73	20.161	69.851	0.309	0.331	0.102
		449.00	No data	21.983	72.098	0.308	0.212	0.065
450–500	Missing interval, mostly water, sand at base	–	–	–	–	–	–	–
500–550	Coarse, yet pasty *Rm* peat with stringy roots and some sand. Core was not full	509.00	–876.05	–	–	–	–	–
	Voids	519.00	–132.33	23.845	68.946	0.428	0.232	0.099
		529.00	141.58	8.090	82.665	0.216	0.533	0.115
		539.00	79.03	5.399	89.582	0.116	0.482	0.056
	Voids	549.00	–55.81	11.551	82.013	0.185	0.358	0.066
550–600	Coarse, yet pasty *Rm* peat with *Diploria* sp. coral hash	559.00	190.92	20.115	71.296	0.340	0.299	0.102
		569.00	811.37	16.084	76.310	0.391	0.321	0.126
		579.00	688.23	36.731	59.047	0.576	0.103	0.059
		589.00	65.97	8.869	86.544	0.149	0.341	0.051
		599.00	–	19.248	75.080	0.332	0.228	0.076
579–629	Overlap with 550–600/repeat of 589	589.00	323.95	14.477	77.659	0.265	0.352	0.093
	Very wet peat, coral, sand/repeat of 599	599.00	91.53	7.729	86.450	0.151	0.430	0.065
	Very wet peat, coral, sand	612.00	1054.80	17.590	75.326	0.321	0.287	0.092
	Very wet peat, coral, sand	623.00	1006.33	36.516	57.119	0.543	0.148	0.081

https://doi.org/10.1017/qua.2017.101 Published online by Cambridge University Press

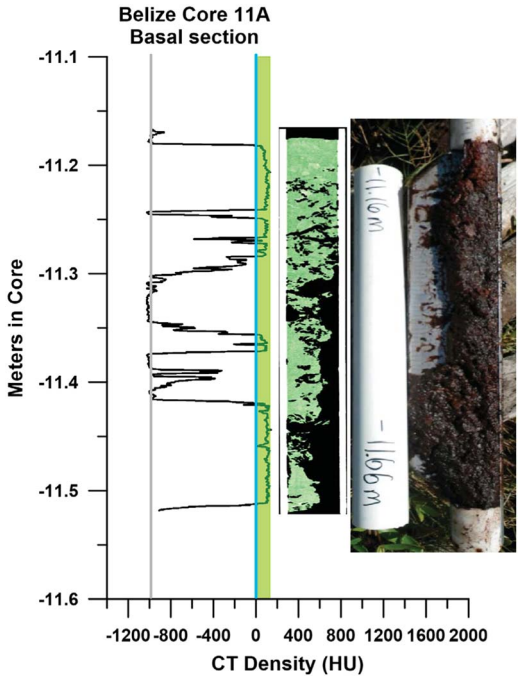

Figure 4. CT density profile of basal section of Belize core 11A, recording large gaps and low-densities, with topogram showing void spaces and field photo showing loose, water-saturated, un-compacted peat at –11.66 m.

CT/LOI/XRD

Through the entire core, *R. mangle* peat exhibited dry bulk densities averaging 0.19 ± 0.03 g cm^{-3} (Fig. 5), similar to the range for Biscayne but over almost twice the depth of that core. LOI/OMC averages 64.9%. CT densities include high negative numbers approaching the density of air (–1000), including at ends of core sections and intervals of low recovery, to a maximum of 155.6 HU near the base of the core. If values (< –800 HU; voids in peat) are removed, the minimum peat density rises to –739.9 HU, and the mean density is –6.6 HU with a standard deviation of 222.13 HU. Removing a wider range of voids (HU < –200) from the calculation yields a mean value of 60.5 HU (~seawater value) for the peat.

Ash yields average 4.97% in the 9.0–9.5 m interval. Water content of the entire core is essentially uniform and very high, averaging 85.8 ± 1.6% (Table 3). Ash-free bulk density averages 0.12 ± 0.02 g cm^{-3} (Table 3), values essentially identical to the shorter section at Biscayne and showing no trend with depth. The 12 m peat section at Belize shows no increase in peat density (via any metric) down core.

Panama

Peat depths to basal/underlying sediments at Panama sites occur over a shallow range of < 1 m, ~20 m inland of the fringe zone, to just >3 m in the fringe zone. In both the Isla Cristobal core at 3.34 m long (Fig. 6), and the Isla Popa core at 2.84 m long (Fig. 7), peat rests on lagoonal carbonate sediments. The deepest 50 cm section of the Isla Cristobal core contained ~30 cm of sediment and *Porites* sp. rubble. We could not core through this underlying sediment with the RPB and do not know if the sediment is basal or an interfingering lens above deeper peat. This core depth is consistent with a core from Isla Cristobal represented in McKee et al. (2007).

CT/LOI/XRD, Isla Cristobal core

The CT and LOI profile in Figure 6 shows consistent peat densities to ~–2.9 m in core where peat transitions into lagoonal carbonates. Samples from 9 and 69 cm (0.09–0.69 m) are pure peat with CT densities (66 and 50 HU) very close to that of seawater (Table 4). Minerals found include halite (90 and 80%), anhydrite (10 and 10%), thenardite (0 and 5%), hematite (5 and 0%), and quartz (3 and 3%). At 119 cm, CT density peaks at 141 HU, likely due to the presence of woody matter or small amounts of sediment. Minerals include hematite (60%), thenardite (30%), and gypsum (<5%).

At 219 cm, the core returns to pure peat with CT density (32 HU) very close to that of seawater and minerals similar to the 9 cm and 69 cm samples (halite 80%, anhydrite 10%, thenardite 5%, and quartz 3%). At 289 cm CT density increases slightly to ~94 HU, halite decreases to 40%. Hematite (25%), quartz (25%) and feldspar (<10%) are present at this depth. In the sediment at 329 cm (Table 4), the highest CT density of 1344 HU occurs with a correspondingly low LOI of 14.3% and with calcite dominating the sediment at 82% of the ash component.

OMC averages 67 ± 5% in the peat section, dropping to 61 ± 10% including the basal sediment (Fig. 6). Ash yields average 7.7%, from a minimum of 3.8% to a maximum of 38.4%, with highest values occurring in the sediment section from 319–329 cm. Water content of the entire core (Table 4) is essentially uniform and very high, averaging 82.8%, apart from the sediment section (55.25%) below 319 cm (Fig. 6). Dry bulk density above the sediment ranges from 0.1 to 0.21 g cm^{-3} (0.13 ± 0.02 g cm^{-3}) while ash-free bulk density ranges from 0.05 to 0.11 ($0.08–0.09 \pm 0.01$ g cm^{-3}), similar to Biscayne and Belize.

CT/LOI/XRD, Isla Popa core

Although of slightly higher density overall than the Cristobal core, CT and LOI profiles of the Popa core in Figure 7 show consistent peat densities to ~–2.7 m in core where peat transitions into lagoonal carbonates. Samples at 9, 89, and 149 cm (0.09, 0.89, 1.49 m) have CT densities very close to that of seawater (~78–100 HU; Table 4). Minerals present at 9 and 89 cm include halite (80%, 75%), hematite (10%, 5%), anhydrite (5%, trace), thenardite (5%), quartz (trace, 15%), plagioclase (trace, 5%), and traces of calcite. At 149 cm (1.49 m) clastic components increase with 50% plagioclase, 30% quartz, 15% hematite, and 5% calcite. CT density of ~660 HU at 279 cm (2.79 m; Table 4) shows a high peak due to the presence of 85% silt-sized calcite grains. Salts include halite 10%, anhydrite 5%, with traces of quartz and hematite. Ash yields average 8.6%, from a minimum of 4.1% to a maximum of 37.8% at 2.79 m (the peat-sediment

https://doi.org/10.1017/qua.2017.101 Published online by Cambridge University Press

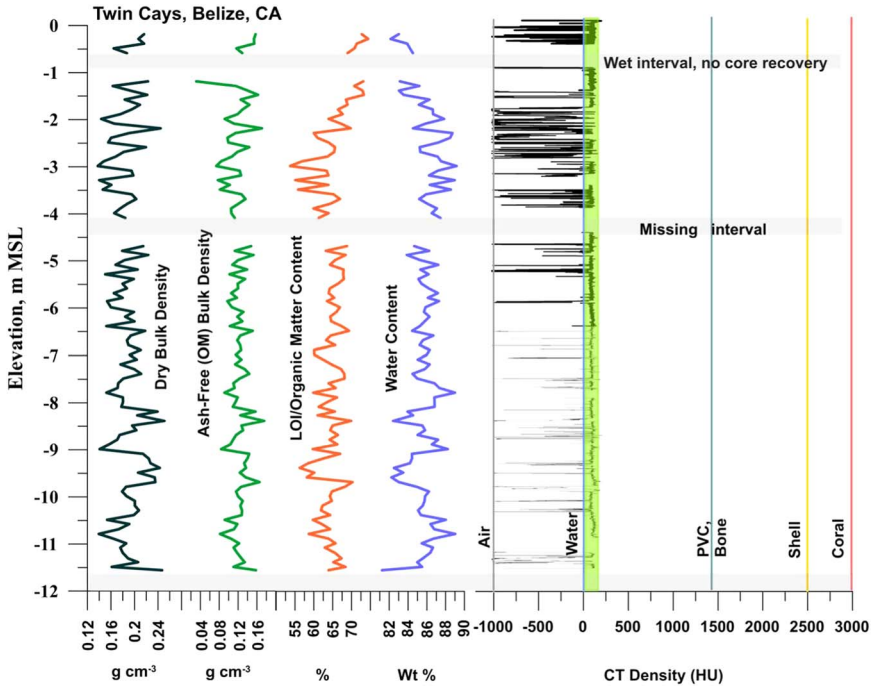

Figure 5. (color online) CT densities and bulk peat analysis for Belize Core 11A. See Figure 2B for selected topogram images. Note the consistent *R. mangle* peat composition over the full 12 m, with no basal sediment or lagoonal material. OM averages 64 ±4%. CT densities are consistent down core, near the upper HU range for seawater (~60 HU). Bulk densities vary but do not trend higher down core. Void (un-compacted) spaces occur at all depths indicated by negative CT densities. Water contents are >80% throughout; note un-cored intervals due to excess water in the peat, and the loose, wet peat at –11.66 m (Fig. 4). Ash-free (OM) bulk densities averaging 0.12 ± 0.02 g cm^{-3} are identical to the 6.3 m Biscayne section and show no trend in peat decomposition or major changes in surface moisture conditions over time.

interface). OMC averages 57 ± 7% in the peat section, dropping to 54 ± 11% including the basal sediment. Water content of the entire core (Fig. 7; Table 4) is essentially uniform and very high, ranging from 58% in the sediment section to 87% in peat, averaging 82%. Dry bulk density above the sediment ranges from 0.11 to 0.25 g cm^{-3} (0.16 ± 0.03 g cm^{-3}) while ash-free (OM) bulk density ranges from 0.07 to 0.12 g cm^{-3} (0.09 ± 0.01 g cm^{-3}), similar to all cores in this study.

Compacted peat CT

Basal Holocene peats from Morrosquillo, Colombia (Fig. 1) were cored from beneath 3–5 m of sand, clay, and peat overburden, a classic setting for compression and dewatering (Bird et al., 2004). Five samples were CT scanned for density profiles and total number of voxels at all HU values. Additional samples from similar depths were analyzed via LOI to characterize these buried peats against the attributes of continuous peats.

CT/LOI compacted peat

Figure 8 shows CT images of Morrosquillo peats with depths in core (= m overburden). Figure 9 plots CT densities measured (in 3-d) on all samples in Figure 8 as a histogram, with all core sections of Belize core 11A. Belize cores plot over the same density range regardless of depth in core, with 12 m appearing as a single peak centered on 75 HU. Morrosquillo samples exhibit a bimodal density distribution with peaks at 175 and 300 HU. Higher CT densities in buried peats are consistent with generally higher LOI values from another sample in this deposit that is depth- and type-correlative to sample XII (Fig. 8) under 4 m overburden (Table 5). Compacted ash-free bulk densities (averaging 18 ± 5 g cm^{-3}) are one to three orders of magnitude higher than continuous peats (~0.15 g cm^{-3}) while dry bulk densities (averaging 0.5 ± 0.2 g cm^{-3}) are similar (~0.10 g cm^{-3}). Compacted water content averaging 62 ± 9% is generally lower than the >80% values for the continuous peats, and comparable to lower values in sediment sections of cores above. OM% ranges from 7–85%, averaging 42 ± 22%, suggesting compaction combined with a sediment component.

Dried peat CT

Air-dried *R. mangle* peat obtained from horizontally stored sections of Tobacco Range, Belize core TR7 (Macintyre et al., 1995) from a 2–4 m depth range (3230 cal BP at –2.5 m MSL; Toscano and Macintyre, 2003) was scanned and densities measured on slices (Table 1) as well as from continuous core-length density profiles (Fig. 10). Drying of the peat occurred due to slow evaporation over long-term storage. CT images of the dried peat show well-preserved large root structures and woody debris in an airy, open matrix

https://doi.org/10.1017/qua.2017.101 Published online by Cambridge University Press

Table 3. Core description, CT densities, and LOI data for Belize Core 11A. *Rm* refers to *Rhizophora mangle* peat.

Belize Core 11A Section (cm)	Core description	Depth in core (cm)	CT HU	Ash content (wt %)	Water content (wt %)	Dry Bulk density (g cm^{-3})	LOI/ OMC	Ash-free (OM) bulk density (g cm^{-3})
0–50	Coarse *Rm* peat; wet	9.00	96.24	4.631	83.019	0.216	0.727	0.157
	Voids	19.00	–109.59	4.564	82.156	0.207	0.744	0.154
	Voids	29.00	–21.14	4.603	83.916	0.216	0.714	0.154
	Peat	39.00	81.86	4.615	84.199	0.165	0.708	0.117
	Voids	49.00	–73.29	4.812	84.508	0.187	0.689	0.129
50–100	Missing interval; too wet to core.	50-100	–	–	–	–	–	–
100–150	*Rm* peat; wet	109.00	97.57	4.530	83.133	0.223	0.148	0.031
		119.00	90.59	4.335	85.202	0.163	0.113	0.115
		129.00	91.37	4.591	83.035	0.193	0.153	0.141
		139.00	97.78	4.403	83.523	0.222	0.120	0.162
		149.00	63.96	4.320	86.277	0.183	0.108	0.126
150–200	*Rm* peat; runny	158.00	90.03	4.614	85.141	0.209	0.139	0.144
		168.00	90.45	4.491	86.627	0.195	0.102	0.130
		179.00	96.57	4.316	86.655	0.176	0.135	0.119
	Voids	189.00	–154.97	4.385	87.850	0.143	0.119	0.092
	Voids	199.00	–436.90	4.641	85.859	0.166	0.120	0.111
200–250	*Rm* peat; runny/voids	209.00	–711.61	4.674	84.529	0.244	0.105	0.171
	Core not full,	219.00	–975.74	4.508	88.730	0.191	0.118	0.115
	air space reflected	229.00	–554.18	4.497	88.491	0.160	0.097	0.098
	in -HU values	239.00	73.43	4.603	87.238	0.155	0.107	0.099
		249.00	–985.88	5.076	85.234	0.219	0.131	0.144
250–300	*Rm* peat; runny	259.00	–822.1	5.082	85.302	0.182	0.118	0.119
		269.00	–193.81	4.675	87.143	0.168	0.129	0.107
		279.00	77.57	5.376	87.527	0.148	0.102	0.084
		289.00	–512.43	5.015	89.168	0.138	0.151	0.074
		299.00	61.96	4.702	87.154	0.195	0.125	0.124
300–350	*Rm* peat; runny	309.00	93.30	4.980	86.221	0.198	0.118	0.126
	Peat	319.00	88.51	4.956	88.968	0.140	0.124	0.077
	Voids	329.00	–269.19	4.949	86.301	0.161	0.126	0.103
	Low recovery	339.00	–	5.053	88.564	0.146	0.115	0.081
	Low recovery	349.00	–	4.899	85.915	0.195	0.127	0.127
350–400	*Rm* peat; less runny	359.00	–681.22	4.898	85.183	0.203	0.114	0.136
		369.00	91.93	4.962	86.059	0.188	0.134	0.121
		379.00	88.01	5.188	87.063	0.176	0.144	0.105
		389.00	29.50	4.864	86.511	0.166	0.123	0.106
	Open end of core	399.00	–964.23	4.858	87.449	0.184	0.110	0.113
400–450	Missing interval	400-450	–	–	–	–	–	–
450–500	*Rm* peat; full recovery; less runny	459.00	87.79	4.791	84.657	0.215	0.091	0.148
		469.00	84.09	5.066	86.241	0.179	0.119	0.113
		479.00	93.73	5.092	83.865	0.223	0.115	0.153
		489.00	94.20	5.051	85.294	0.183	0.109	0.120
	Sampled prior to CT	498.00	–	4.561	87.229	0.168	0.157	0.108
500–550	*Rm* peat; same	509.00	85.70	4.721	85.300	0.205	0.125	0.139
		519.00	85.16	4.450	86.183	0.150	0.176	0.102
		529.00	–186.76	4.772	85.101	0.199	0.127	0.135
		539.00	75.44	4.894	85.427	0.180	0.131	0.119
		549.00	97.51	4.932	86.201	0.187	0.116	0.120
550–600	*Rm* peat; same	559.00	86.04	4.620	87.184	0.165	0.109	0.105
		569.00	–17.49	4.809	86.095	0.180	0.104	0.118
		579.00	101.00	4.636	87.302	0.153	0.084	0.097
		589.00	140.98	4.681	85.843	0.160	0.144	0.107
		596.00	69.21	4.865	85.694	0.199	0.140	0.131
600–650	*Rm* peat; same	609.00	88.55	4.893	86.271	0.184	0.133	0.118
		619.00	91.07	5.034	85.760	0.200	0.137	0.129
		629.00	100.87	4.812	85.256	0.152	0.124	0.102
		639.00	103.20	4.773	84.432	0.218	0.136	0.151

https://doi.org/10.1017/qua.2017.101 Published online by Cambridge University Press

Table 3. (*Continued*)

Belize Core 11A Section (cm)	Core description	Depth in core (cm)	CT HU	Ash content (wt %)	Water content (wt %)	Dry Bulk density (g cm^{-3})	LOI/ OMC	Ash-free (OM) bulk density (g cm^{-3})
	At 648	649.00	105.28	4.730	86.690	0.194	0.166	0.125
650–700	*Rm* peat; same	659.00	–538.18	5.302	85.567	0.187	0.127	0.118
		669.00	99.87	5.072	85.226	0.190	0.116	0.124
		679.00	82.70	5.470	86.298	0.211	0.120	0.126
		689.00	–485.65	5.587	85.980	0.192	0.130	0.115
	At 698	699.00	45.13	5.616	85.025	0.204	0.125	0.127
700–750	*Rm* peat; same	709.00	84.18	4.846	86.289	0.176	0.128	0.114
	486 mm recorded	719.00	90.19	4.661	85.775	0.199	0.128	0.134
		729.00	78.81	4.956	84.471	0.211	0.092	0.144
		739.00	91.15	4.783	84.983	0.181	0.119	0.123
	At 748	749.00	95.08	4.762	86.804	0.172	0.111	0.110
750–800	*Rm* peat; same	759.00	91.56	4.333	87.329	0.171	0.082	0.113
		769.00	82.67	4.418	89.001	0.152	0.105	0.091
		779.00	94.33	4.470	86.788	0.180	0.122	0.119
		789.00	–9.97	4.811	86.808	0.180	0.111	0.115
	795 deepest record	799.00	77.31	5.104	86.815	0.178	0.118	0.109
800–850	*Rm* peat; same	809.00	88.82	5.525	83.941	0.239	0.127	0.157
		819.00	91.14	6.033	84.531	0.205	0.134	0.125
		829.00	91.00	5.290	82.409	0.251	0.110	0.176
		837.00	96.48	5.071	85.520	0.196	0.158	0.127
	(Space at base of core)	849.00	–969.76	5.059	85.808	0.203	0.148	0.131
850–900	*Rm* peat; same	859.00	101.23	5.036	85.012	0.175	0.113	0.116
	467.7 mm recorded	869.00	114.65	4.585	87.202	0.171	0.153	0.109
		879.00	138.52	4.548	86.528	0.157	0.120	0.104
		889.00	104.31	4.737	88.238	0.141	0.108	0.084
	(Space at base of core)	899.00	–	5.144	84.414	0.214	0.139	0.144
900–950	*Rm* peat; same	909.00	97.14	5.843	84.418	0.224	0.102	0.140
		919.00	93.08	6.549	84.204	0.227	0.135	0.133
		929.00	94.46	7.650	82.501	0.243	0.119	0.137
		939.00	–287.73	6.586	83.488	0.206	0.120	0.124
	947 deepest CT	949.00	90.43	7.436	82.235	0.234	0.105	0.136
950–1000	*Rm* peat; same	959.00	–571.52	5.051	83.010	0.236	0.118	0.166
		969.00	104.13	4.793	84.913	0.186	0.097	0.127
		979.00	126.06	4.853	86.216	0.179	0.107	0.116
		989.00	128.86	5.074	85.804	0.186	0.131	0.120
	998 deepest CT	999.00	155.61	5.020	85.753	0.201	0.118	0.130
1000–1050	*Rm* peat; same	1009.00	77.58	5.444	85.559	0.201	0.129	0.125
	485 mm recorded	1019.00	–739.95	5.691	85.065	0.207	0.102	0.128
		1029.00	84.05	5.218	85.365	0.199	0.151	0.128
		1039.00	44.73	4.819	88.028	0.153	0.125	0.092
	1048 deepest CT	1049.00	94.84	5.163	86.377	0.191	0.118	0.119
1050–1100	*Rm* peat; same	1059.00	107.23	4.713	86.783	0.173	0.124	0.111
	472 mm recorded	1068.00	114.22	4.538	89.024	0.139	0.126	0.082
		1079.00	110.30	4.797	86.703	0.164	0.115	0.105
		1089.00	126.57	4.983	85.449	0.186	0.127	0.122
	1097 deepest CT	1099.00	107.56	4.958	86.638	0.176	0.114	0.111
1100–1150	*Rm* peat; same	1109.00	–	4.698	86.358	0.180	0.134	0.118
		1118.00/1119.00	94.13	4.712	85.565	0.189	0.144	0.127
	353.45 mm recorded	1129.00	–713.97	5.232	84.979	0.206	0.123	0.134
	No CT	1141.00	–146.12	4.584	85.485	0.161	0.110	0.110
	No CT	1149.00	113.23	6.770	81.238	0.247	0.113	0.158
1116–1166, overlaps above	*Rm* peat; medium recovery, very wet and loose	1159.00	–	–	(>90%)	–	–	–
	samples taken in bags, No CT/LOI data	1166.00	–	–	(>90%)	–	–	–

https://doi.org/10.1017/qua.2017.101 Published online by Cambridge University Press

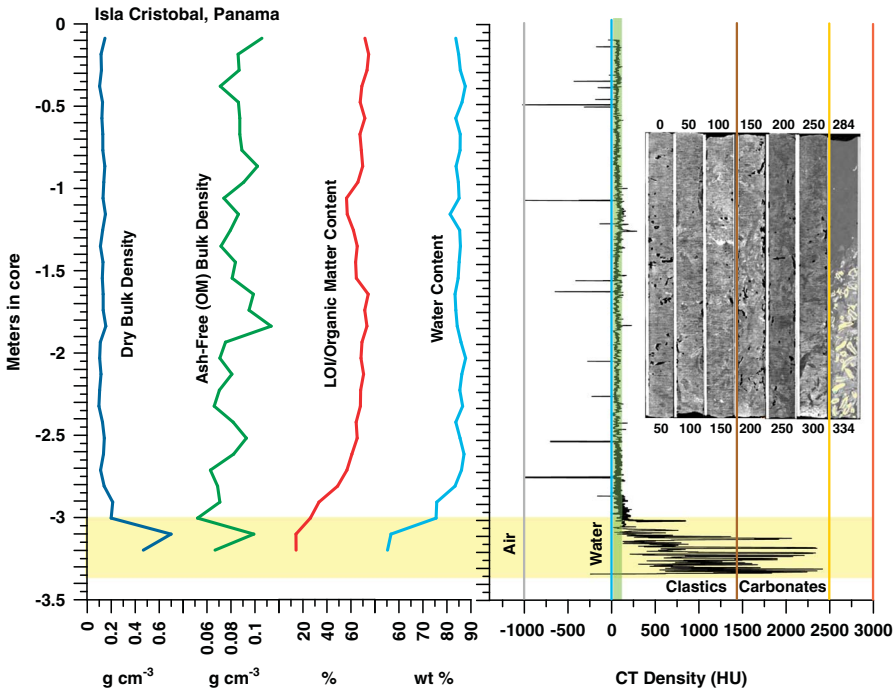

Figure 6. (color online) Graph of CT and bulk peat densities, LOI, and H_2O content analysis and CT topogram images for the Cristobal, Panama core. OMC averages 67 ± 5% in the peat section. CT densities are slightly higher in this short core compared to Belize and Biscayne, possibly due to the presence of minor terrigenous and carbonate sediment in the peat. The peats exhibit no trend in CT or bulk density with depth. High densities at the bases of cores reflect the lagoonal sediment and coral underlying the peat. Water content in peat is uniformly >80%, dry bulk density is uniformly low (0.13 ± 0.02 g cm^{-3}), and ash-free organic matter OM bulk density (0.09 ± 0.01 g cm^{-3}) is consistent with Biscayne and Belize.

of fine surface roots (Fig. 10), indicating preservation of the original peat-forming substrate and spatial relationships with no visible packing, flattening, or loss of open root structure. Average CT densities were consistently below –500 HU, indicating that the dried sections consist of >50% air space in the material.

DISCUSSION (IMPLICATIONS FOR SEA LEVEL STUDIES)

Determining the degree of peat compaction via direct density measurements (CT), physical (core), visual (images), and proxy (BDs and water contents) data is a necessary step in understanding and possibly reducing one major area of uncertainty in assigning elevations to sea-level index points. The measurements of physical parameters in this study currently stand alone and have not yet been combined with geochemical indicators of decay or peat disturbance (such as C/N profiles and anomalies) that may indicate impacted peat ages. Density profiles and water contents cannot account for, or preclude, bioturbation, hiatuses, younger root contamination of underlying deposits, and remobilization of older peat carbon by younger roots. Our data do shed light on the subsurface hydrologic environment of open-ocean, sediment-starved peat sequences and the role of seawater saturation, tidal forces, and hydraulic pressure or conductivity in supporting and maintaining paleo peat elevations over millennia of sea-level rise.

In Belize and the Florida Keys, mangroves became established on shelf-edge Pleistocene carbonate banks after Holocene SLR reached the elevations of these sites (e.g., Robbin, 1984; Toscano and Lundberg, 1998; Macintyre et al., 2004), and have accumulated peat to the present. Panamanian mangroves in the Bocas del Toro Archipelago were established on shallow carbonate lagoonal sediments around heavily vegetated clastic islands. Belize mangrove sites are 24 km offshore and receive essentially no mainland-derived sediment (Koltes and Opishinksi, 2009), whereas in Florida, over the limited aerial extent of our core site, some pre-transgression, mainland-derived quartz sediment occurs in deeper sections of the peat above the Key Largo Limestone basement. At all sites, there is virtually no within-mangrove carbonate production apart from scattered cerithid gastropods and intertidal foraminifera, neither of which are preserved in subsurface peat, likely due to dissolution (e.g., Green et al., 1998). Bulk biogenic carbonate sediment, produced in surrounding shallow lagoons, occurs as thin basal sediment or as localized facies incursions into mangrove sequences (Macintyre et al., 1995, 2004). Uninterrupted, pure mangrove peat sequences have accreted over time in direct response to local-relative SLR through biotic mechanisms, with no assistance from incremental sediment inputs (McKee et al., 2007; McKee, 2011). Holocene accretion is represented

https://doi.org/10.1017/qua.2017.101 Published online by Cambridge University Press

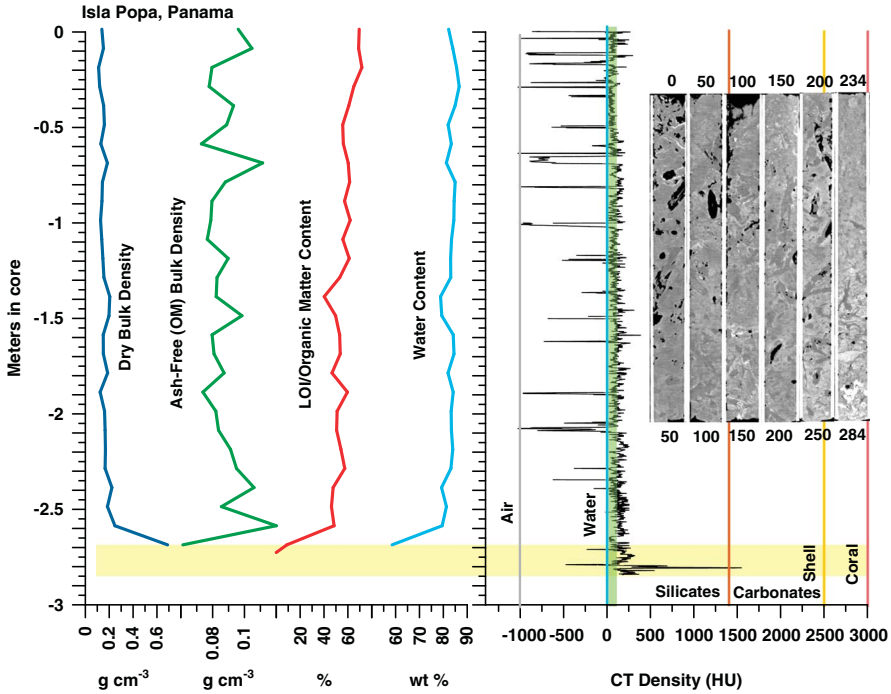

Figure 7. (color online) Graph of CT and bulk peat analysis and CT topogram images for Popa, Panama core. OMC averages 57 ± 7%, somewhat lower than other cores, and CT densities are higher than in the Cristobal core, likely due to the presence of terrigenous and carbonate sediment in the peat, or more woody components. Despite the higher density overall, the peat section exhibits virtually no trend in density with depth. High densities at the base of the peat reflect the underlying lagoonal sediment and coral. Water content in the peat section above the sediment is uniformly >80%, dry bulk density is uniformly low (0.16 ± 0.03 g cm^{-3}), and ash-free (OM) bulk density is (0.09 ± 0.01 g cm^{-3}) is consistent with all other cores in this study.

solely by high (>80%) water content peat, whose thickness reflects the depth to basement, from –7.5 to >–12 m in Belize, >–6.5 to –1.5 m in the Florida Keys, and up to 3.5 m over basal coral-rich sediment in Panama.

RPB coring, which produces open half cores, clearly reveals peat wetness and lack of compression during the coring, including the intervals of no recovery due to excessive water mentioned above. Thus, despite our recognition of compaction for all pertinent reasons, our field observations of mangrove peat do not indicate dewatering and compression at any depth or at any site.

All of our offshore mangrove island sites have in common both the preservation of identifiable peat components (particularly refractory fine roots), persistence of voids at all depths, and consistently high water contents from surface to basement in these peat sequences regardless of thickness. Similarly, dry bulk densities, ash-free bulk densities and CT densities are consistent among sites and minimally variable down the full lengths of all cores, showing no trends of increasing density with depth regardless of peat thickness. Progressively increasing peat density and decreasing pore space and water content with depth, all primary indicators of compaction, are not observed in these sediment-free peat sections. In Belize, where the thickest peat sections occur, Monacci et al.'s (2009) peat core BT-79 from Spanish Lookout Cay similarly exhibited consistently low and minimally variable dry bulk density ranges (8 m; 0.12 ± 0.02 g cm^{-3}) similar to core 11A on Twin Cays (11.66 m; 0.19 ± 0.26 g/cm^3). Ash-free bulk densities in BT-79 averaging 0.12 ± 0.02 g cm^{-3} were identical to core 11A and showed no trend with depth. Ash-free bulk densities from shorter peat sections in Biscayne core 6A (4 m; 0.11 ± 0.03 g/cm^3), Cristobal (3 m; 0.09 ± 0.01 g/cm^3) and Popa (3 m; 0.09 ± 0.01 g/cm^3) are essentially the same as in Belize (0.12 ± 0.02 g cm^{-3}), which is almost twice the thickness of the Biscayne peat and four times the thickness of the Panama peats. These values are consistent with ash-free bulk densities in continental ombotrophic peats, falling closer to the lowest values (~0.08 g cm^{-3}) that signify well-preserved identifiable plant components accumulated more rapidly in a wet environment (such as a tidal mangrove), than to the highest values (0.2 g cm^{-3}), which signify more decomposed and unidentifiable peats formed more slowly under drier conditions (Yu et al., 2003). Ash-free bulk density might therefore be used as a rough proxy for variation in the degree of total peat decomposition correlated to surface moisture conditions over time, which, in the case of intertidal mangrove fringe zones, is consistently high. Monacci et al. (2009) specifically state that the relatively uniform bulk densities in their core indicate compaction was not significant and unlikely to have influenced the elevations of dated samples used in sea-level interpretation. Bird et al.'s (2004) compaction experiments were conducted on highly complex peat and sediment sequences, including peats under

https://doi.org/10.1017/qua.2017.101 Published online by Cambridge University Press

Table 4. Core description, CT densities, and LOI data, Panama Isla Cristobal and Isla Popa cores. *Rm* refers to *Rhizophora mangle* peat.

Isla Cristobal Core Section (cm)	Core Description	Depth in core (cm)	CT HU	Ash content (wt %)	Water content (wt %)	Dry Bulk Density (g cm^{-3})	LOI/ OMC	Ash-free (OM) bulk density (g cm^{-3})
0–50	*Rm* peat	9.00	65	4.622	83.690	0.148	0.717	0.106
	Rm peat	19.00	50	3.816	84.877	0.115	0.748	0.086
	Rm peat	29.00	14	3.834	85.583	0.118	0.734	0.087
	Rm peat	39.00	46	3.820	87.649	0.103	0.691	0.071
	Rm peat	49.00	51	4.424	86.299	0.127	0.677	0.086
50–100	*Rm* peat	59.00	60	4.636	83.680	0.122	0.716	0.087
	Rm peat	69.00	51	4.698	85.551	0.129	0.675	0.087
	Rm peat	79.00	58	4.547	85.488	0.130	0.687	0.089
	Rm peat	89.00	79	4.890	83.814	0.146	0.698	0.102
	Rm peat	99.00	57	5.216	84.760	0.138	0.658	0.091
100–150	*Rm* peat	109.00	90	6.524	85.069	0.132	0.563	0.074
	Rm peat	119.00	57	8.042	81.327	0.151	0.569	0.086
	Rm peat	129.00	83	5.571	85.313	0.128	0.621	0.080
	Rm peat	139.00	46	4.994	85.627	0.110	0.653	0.072
	Rm peat	149.00	53	5.385	85.089	0.131	0.639	0.084
150–200	*Rm* peat	159.00	86	5.438	84.678	0.126	0.645	0.081
	Rm peat	169.00	43	4.255	83.378	0.133	0.744	0.099
	Rm peat	179.00	66	4.644	83.707	0.133	0.715	0.095
	Rm peat	189.00	57	4.187	84.297	0.155	0.733	0.113
	Rm peat	199.00	83	4.354	85.867	0.109	0.692	0.075
200–250	*Rm* peat	209.00	53	3.860	87.793	0.103	0.684	0.071
	Rm peat	219.00	33	4.064	86.212	0.115	0.705	0.081
	Rm peat	229.00	78	4.667	85.373	0.103	0.681	0.070
	Rm peat	239.00	45	4.323	86.542	0.097	0.679	0.066
	Rm peat	249.00	81	5.811	83.700	0.127	0.643	0.082
250–300	*Rm* peat	259.00	82	5.054	85.469	0.142	0.652	0.093
	Rm peat	269.00	62	5.051	87.121	0.135	0.608	0.082
	Rm peat	279.00	52	6.039	86.072	0.111	0.566	0.063
	Peat/sediment	289.00	111	8.498	83.377	0.141	0.489	0.069
284–334	*Rm* peat	299.00	94	16.162	75.758	0.212	0.333	0.071
	Carbonate lagoonal sediment	309.00	664	18.108	75.476	0.199	0.262	0.052
	Carbonate lagoonal sediment	319.00	1964	37.171	56.689	0.699	0.142	0.099
	Carbonate lagoonal sediment	329.00	1344	38.367	55.245	0.468	0.143	0.067
Isla Popa Core Section (cm)								
0–50	*Rm* peat	9.00	79	5.423	82.215	0.138	0.695	0.089
	Rm peat	19.00	64	4.972	83.963	0.152	0.690	0.073
	Rm peat	29.00	–245	4.084	85.55	0.111	0.717	0.111
	Rm peat	39.00	39	4.680	86.650	0.120	0.649	0.088
	Rm peat	49.00	–41	5.913	84.928	0.153	0.608	0.080
50–100	*Rm* peat	59.00	–40	7.983	81.996	0.160	0.557	0.079
	Rm peat	69.00	110	7.290	83.345	0.130	0.562	0.077
	Rm peat	79.00	140	7.437	81.272	0.185	0.603	0.090
	Rm peat	89.00	79	5.799	84.949	0.143	0.615	0.083
	Rm peat	99.00	144	6.622	84.532	0.139	0.572	0.082
100–150	*Rm* peat	109.00	67	5.936	84.402	0.127	0.619	0.098
	Rm peat	119.00	–90	7.327	83.437	0.137	0.558	0.080
	Rm peat	129.00	116	6.588	83.044	0.147	0.611	0.081
	Rm peat	139.00	111	7.908	83.109	0.156	0.532	0.087
	Rm peat	149.00	101	12.666	78.829	0.205	0.402	0.074
150–200	*Rm* peat	159.00	92	10.388	79.349	0.198	0.497	0.082
	Rm peat	169.00	102	7.432	84.149	0.150	0.531	0.084
	Rm peat	179.00	148	7.207	84.467	0.151	0.536	0.091
	Rm peat	189.00	–97	9.618	81.962	0.187	0.467	0.095
	Rm peat	199.00	142	6.406	84.128	0.124	0.596	0.106
200–250	*Rm* peat	209.00	103	8.195	83.278	0.161	0.510	0.086
	Rm peat	219.00	78	8.210	83.395	0.166	0.506	0.120

https://doi.org/10.1017/qua.2017.101 Published online by Cambridge University Press

Table 4. (*Continued*)

Isla Cristobal Core Section (cm)	Core Description	Depth in core (cm)	CT HU	Ash content (wt %)	Water content (wt %)	Dry Bulk Density (g cm^{-3})	LOI/ OMC	Ash-free (OM) bulk density (g cm^{-3})
	Rm peat	229.00	124	7.353	83.943	0.168	0.542	0.061
	Rm peat	239.00	79	7.167	83.183	0.166	0.574	0.096
	Peat/sediment	249.00	188	10.862	79.254	0.223	0.476	0.105
234-284	Peat/sediment	259.00	156	10.056	81.292	0.185	0.462	0.080
	Peat/sediment	269.00	155	10.565	79.513	0.248	0.484	0.078
	Peat/sediment	279.00	660	37.761	58.547	0.689	0.089	0.093
	Carbonate lagoonal sediment	283.00	239	–	–	–	–	–

sediments, around Singapore in order to estimate the amount of compaction of any sediment or peat interval based essentially on the difference between initial bulk density (modern/surface, 0–5 cm) and compacted bulk density (fossil/subsurface, 15–20 cm). Our core sequences are comparatively uncomplicated, with no sediment intervals to compress the underlying peat and microtidal ranges limiting the degree of peat exposure and draining. In addition, our direct CT measurements of peat density and sample bulk densities demonstrate that density does not increase with depth. Water contents remain very high through the peat sections, with no decreasing trend with depth, as would be predicted by the assumption of compaction. In contrast, our peat samples from Colombia, taken from beneath several m of sediment, show up to three orders of magnitude higher ash-free BDs than continuous peats, as well as higher dry bulk densities, and lower water contents (~67% vs >80%). In addition, our dried-peat images and data indicate that peat maintains its open root structure, exhibits the negative CT densities of the observed air spaces, and shows no visual or quantitative evidence of compaction.

In sediment-free *R. mangle* peat, fine surface root production parallels surface litter production indicating healthy stands with high productivity, specifically in fringe zones (McKee et al., 2007). Leaves and other aboveground materials undergo fragmentation and some decomposition before burial, while roots produced in an anaerobic environment are well preserved (Middleton and McKee, 2001; McKee et al., 2007; McKee, 2011). Roots were well preserved in another of our long cores to 10 m basal depths, representing up to 90% of the peat throughout the section. McKee and Faulkner (2000) determined that Cat Cay, Belize, has expanded horizontally and vertically through belowground, biogenic processes, with mangrove roots playing a critical role in peat formation and vertical accretion of oceanic mangrove cays. In Belize, the only one of our sites with Rod-Surface Elevation Table (RSET) measurements of peat elevation changes relative to benchmark depths over a 3-yr period. McKee et al. (2007) found

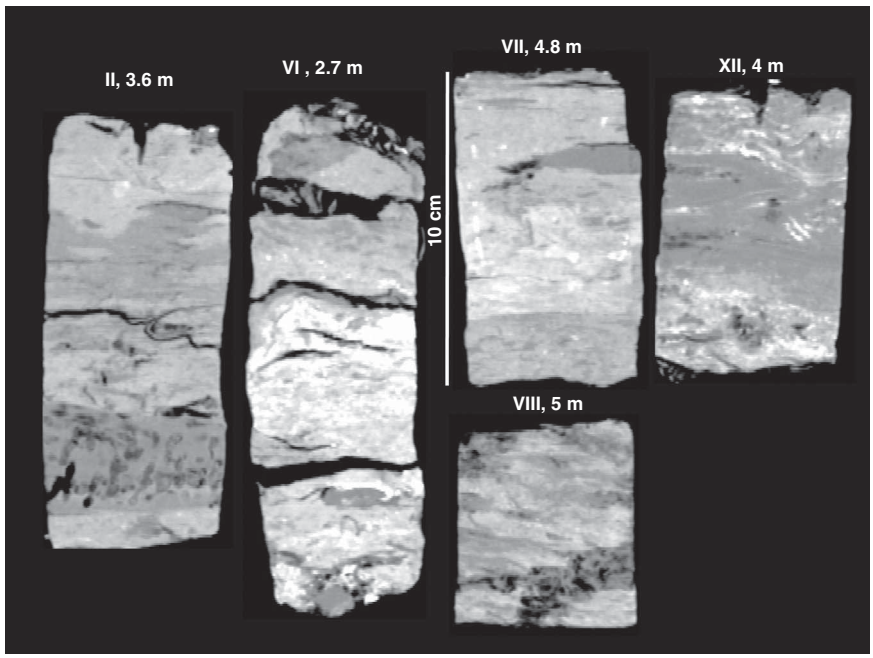

Figure 8. CT images of buried peats from Morrosquillo, Colombia, with depths below the surface (= m of sediment overburden).

https://doi.org/10.1017/qua.2017.101 Published online by Cambridge University Press

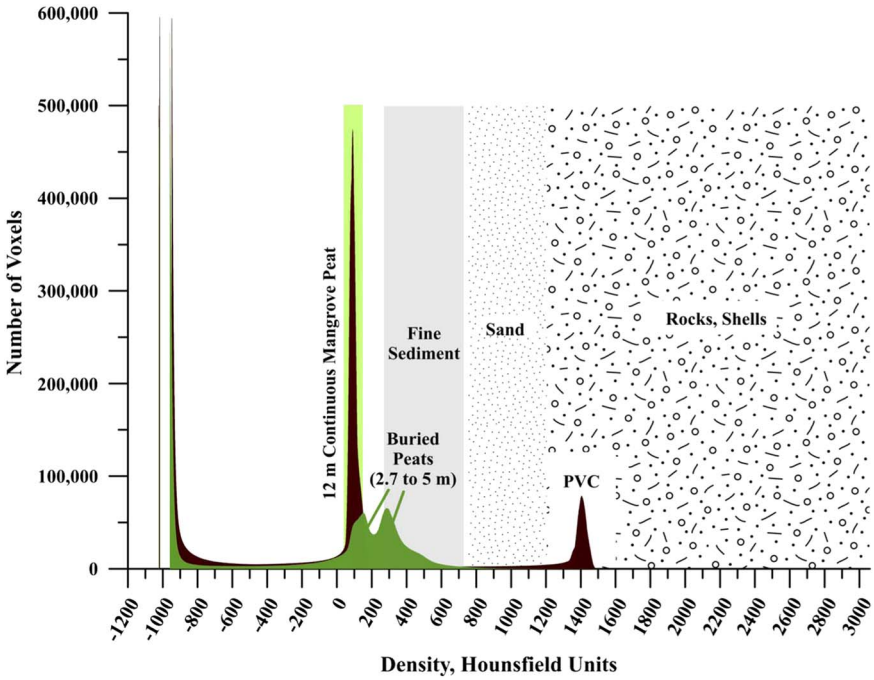

Figure 9. (color online) Three-dimensional analysis of all voxels counted from Morrosquillo peats, showing bimodal density peaks at 175 and 300 HU. For comparison, all core sections spanning the 12 m of continuous Belize core 11A are plotted, within a single peak (all sections overlapping) centered on 75 HU. Note PVC core liner peak at 1400 HU. The shift to higher HU values in the buried peats is likely a combination of overburden-forced compaction and dewatering and a minor sediment component in this area. See Table 5 for LOI analysis of the buried peat. Sediment HU ranges are from the analysis of Davey et al. (2011).

trends ranging from -3.7 mm yr^{-1} (interior dwarf/pond) to +4.1 mm yr^{-1} (fringe). The interior dwarf/pond facies is a hypersaline, high-stress environment with slow growing dwarf *R. mangle* trees and low rates of peat (root and litter) accumulation, while the fringe zone is on the leading edge of SLR and allochthonous nutrient inputs (Feller et al., 2003), supporting the positive 3-yr elevation change rate which is of the same order of magnitude as the rate of local relative SLR. The rate of Holocene peat accumulation must likewise include peat productivity variations resulting from lateral migration of dwarf, transition, and fringe zones across core sites through time, and many possible but undetectable interruptions in peat deposition, including hiatuses due to mangrove diebacks (Cahoon et al., 2003) and changes in the rate of SLR. In addition, processes occurring in deeper peat may have an effect on elevation change of the peat surface (Cahoon and Lynch, 1997; Cahoon et al., 2003; Whelan et al., 2005; McKee et al., 2007).

Surface litter is lost from the mangrove through tidal exportation, microbial decomposition, and detrivory (Middleton and McKee, 2001; Ono et al., 2006), which indicate that mangrove roots are the primary component of peat (Cameron and Palmer, 1995; McKee and Faulkner, 2000). Over a short (1 m) *Rhizophora* spp. peat profile, Ono et al. (2015) showed via closely-spaced ^{14}C dating that modern fine roots penetrated to at least ~80 cm, indicating the importance of high production of mangrove fine roots to peat accumulation. Indeed, our dried peat CT scans clearly show the preservation of the open structure of the surface fine root systems making up the framework of the peat, precluding any possibility of compression and compaction. The air spaces are filled with water in wet peat, indicating that water pressure maintains the spaces between the roots and exerts sufficient multidirectional pressure throughout the system to prevent compaction and compression.

Mangrove surface water flows through established tidal channels and across prop roots (Mazda et al., 2005; Urish et al., 2009). Subsurface water flow through unsaturated peat is affected by irregular pore structure (Rezanezhad et al., 2009) and effective porosity, assuming decreases in porosity with depth and increasing decomposition and increases in bulk density. However, subsurface hydraulic conductivity increases with increasing organic content (Kolay and Shafiee, 2007). Hansson et al. (2013) compared bulk density and other proxies for decomposition in an ombotrophic peat and observed that the portion of the deposit situated below the lowest water table is permanently saturated and supported by water, and cannot be further compacted. When supporting water is removed from the deposit via drainage (Kolay and Shafiee, 2007) or decreases naturally (Whelan et al., 2005), the peat surface subsides. In the Everglades, Whelan et al. (2005) positively correlated the rate of change of groundwater head pressure (from river stage, tidal influences, and seasonal changes in river discharge) to the RSET-measured rate of change in peat surface elevation for the complete peat section in which peat swelled in response to hydrological recharge and subsided in response to lowered groundwater

https://doi.org/10.1017/qua.2017.101 Published online by Cambridge University Press

Table 5. LOI data, Morrosquillo, Colombia basal peat section 152005 below 4 m siliciclastic overburden. Sample is correlative to CT-scanned sample XII in Figure 8.

Morrosquillo XII depth in core (cm)	Core description	Water content (wt %)	Dry Bulk Density (g cm^{-3})	LOI/OMC	Ash-free (OM) bulk density (g cm$^{-3)}$
420	Compacted peat	73.595	0.197	85.161	16.807
430	Compacted peat	68.941	0.388	52.131	20.245
440	Compacted peat	65.046	0.439	46.667	20.499
450	Compacted peat	61.319	0.500	37.150	18.589
460	Compacted peat	50.313	0.708	18.345	12.987
470	Compacted peat	69.632	0.326	72.656	23.682
480	Compacted peat	64.731	0.425	52.994	22.536
490	Compacted peat	51.591	0.736	19.550	14.388
500	Compacted peat	67.562	0.415	53.988	22.409
510	Compacted peat	65.575	0.442	57.061	25.210
520	Compacted peat	68.298	0.396	56.913	22.536
530	Compacted peat	67.897	0.399	54.633	21.772
560	Compacted peat	56.934	0.601	15.466	9.295
570	Compacted peat	57.900	0.587	19.957	11.714
580	Compacted peat	65.293	0.442	41.727	18.462
590	Compacted peat	54.970	0.663	17.850	11.841
600	Compacted peat	40.055	1.105	6.912	7.639

pressure. The majority of the expansion occurred in deeper zones of peat directly above the underlying bedrock. In the continuously saturated, sediment-starved oceanic peats at our sites, subsurface water is the key environmental component supporting the uncompressed peat structure and vertical integrity up to 12 m depth. Saturation is maintained from the top of cored intervals at all sites where the peat surfaces lie within a microtidal (~15 cm) range.

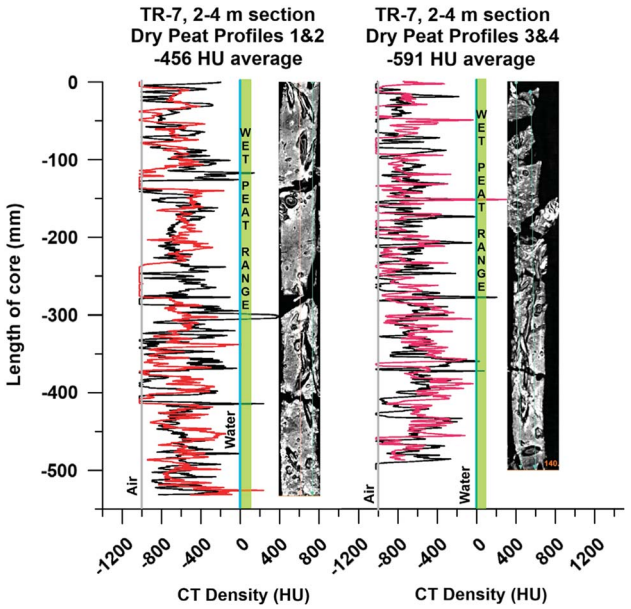

Figure 10. (color online) Dried peat CT density profiles, core TR-7 (2–4 m interval, ~3 ka old), Tobacco Range, Belize (Macintyre et al., 1995). Density profiles 1 and 2 (left) and 3 and 4 (right) with corresponding CT topograms, showing uncompressed preservation of the fine root matrix and open structures of larger roots and voids in the peat. The dominance of air spaces and negative CT densities (~–500 HU) midway between Water (0.0 HU) and Air (–1000 HU) indicate that the water in fresh, waterlogged *R. mangle* peat fills void spaces and defines its general density throughout the deposit.

Despite the demonstrated lack of compaction in *R. mangle* peats in this study, these deposits must still be approached with a wider range of geochemical and physical data to be successfully used in sea-level studies. Peats have undergone aerobic decomposition in the surface litter and likely further fragmentation and diagenesis over time, as well as incorporating signatures of physical disturbances (e.g., storms, bioturbation by crabs, and mangrove diebacks) that are not necessarily discernable from visual inspection or CT imaging of cores. If a mangrove dieback occurred within the peat sequence, the resulting cessation of root production and increase in surface decomposition will incorporate decreases in peat elevation ("peat collapse") until the rate of new root production from surviving and new mangrove trees eventually recovers. Assuming peat elevations are not lowered by compaction or collapse, ^{14}C age inconsistencies (ubiquitous in previous cited studies with ^{14}C dating of peat), particularly the common problem of age reversals, may be attributed to the remobilization of older carbon into younger deposits by penetrating root systems as well as to younger, large root contamination of older peat (McKee, 2001, 2011; Ono et al., 2015). McKee (2001) discusses the proliferation of roots into old root channels in mangrove peat as a means of nutrient conservation in oligotrophic environments, thereby mixing younger and older peat, while Ono et al. (2015) documented an 80 cm depth of penetration of modern fine roots into underlying peat. Peat C/N ratios decline with depth as carbon is lost due to decomposition (Malmer and Holm, 1994) but

https://doi.org/10.1017/qua.2017.101 Published online by Cambridge University Press

anomalously high C/N ratios occurring possibly as a result of mixing of younger material into older peat may account for out of sequence or reversed ^{14}C ages (e.g., Hansson et al., 2013, citing Kuhry and Vitt, 1996). C/N may therefore provide a diagnostic for disturbed or mixed samples to avoid in ^{14}C dating of peat.

CONCLUSIONS

Where peat deposits on offshore platforms are not interrupted by sediment lenses, we found that local hydrology, buoyancy, and tidal forces maintain water pressure throughout well-preserved subsurface root systems. These processes prevent dewatering and subsidence or compaction of continuous peats, and, barring undetected hiatuses, it is highly likely that peat captures paleo-sea level at any depth within the deposit. Down-core CT data, particularly in dried peat cores, are diagnostic of structural preservation of non-compacted root systems and the prevalence of air spaces throughout thick peats where water once maintained the original root spacing. Integration of CT density profiles, bulk densities, and high water contents indicate multi-variate consistencies with depth, contrary to the basic assumptions of compaction due to overburden pressure resulting in increased density and dewatering. Peat does not create its own overburden because it is supported by interstitial water and hydrostatic pressure. CT and bulk density of peats do not vary down cores in this study; thus if CT is not available, bulk density profiles alone are reliable indicators of peat compaction.

While non-compacted peat elevations are most likely reliable, mangrove peat remains a complex proxy for paleo-sea-level reconstructions. RSET-measured rates of peat accretion or subsidence are useful for understanding hydrologic processes affecting peat elevations in specific depositional settings. Other factors affecting accurate sea level indicator status of non-compacted peat include hiatuses in peat formation, peat decomposition processes, and ^{14}C dating errors and age reversals. Our density data show that *R. mangle* peat maintains high water content and hydrostatic pressure at all depths, preventing dewatering and compaction and maintaining the original sea-level-indicative elevation range of any sample at depth. Thick, non-compacted peat sections can potentially provide a continuous proxy for the full site history of SLR, particularly at open ocean platform sites where the basal peat/bedrock depth range is limited.

ACKNOWLEDGMENTS

Funding was provided by NSF (0921879 Toscano), the Smithsonian Caribbean Coral Reefs Ecosystem and MarineGEO Programs (Toscano), and the Halliburton Foundation (Gonzalez). We thank the National Park Service for park-assigned Permit BISC-2012_SCI-0010 (Study No. BISC-00013); Michelle Prats, NPS Intern, and the University of Miami Broad Key Research Station. Sampling and export permits were processed by Belize Fisheries and ARAP, Panama. Dr. Patricia Tester, Christopher Holland (NOAA NMF), J. Hootman, E. and B. James, T.B. Opishinski and Z. Foltz (Carrie Bow Cay, Belize Station Managers), and Eric Brown, Bocas del Toro, Panama, provided field and logistical assistance. Dr. James Hinthorne (UTRGV, U.S. Army Research Office Grant W911NF-08-1-0353) and students Cruz Quintana, Emmanuel Higa, and Eli Gonzalez performed XRD and some LOI analysis. Ilka C. Feller provided a comprehensive review of the manuscript, which was further improved by the comments of anonymous reviewers.

REFERENCES

Allaway, W.G., Curran, M, Hollington, L.M., Ricketts, M.C., Skelton, N., 2001. Gas space and oxygen exchange in roots of *Avicennia marina* (Forssk.) Vierh. var. *australasica* (Walp.) Moldenke ex N.C. Duke, the Grey Mangrove. *Wetlands Ecology and Management* 9, 211–218.

Allen, J.R.L., 2000. Morphodynamics of Holocene salt marshes: A review sketch from the Atlantic and southern North Sea coasts of Europe. *Quaternary Science Reviews* 19, 1155–1233.

Amos, C.L., Sutherland, T.F., Radzijewski, B., Doucette, M., 1996. A rapid technique to determine bulk density of fine-grained sediments by X-ray computed tomography. *Journal of Sedimentary Research* 66, 1023–1024.

Bindoff, N.L., Willebrand, J., Artale, V., Cazenave, A., Gregory, J., Gulev, S., Hanawa, K., et al., 2007. Observations: Oceanic Climate Change and Sea Level. In: Intergovernmental Panel on Climate Change, *Climate Change 2007 - The Physical Science Basis*. Cambridge University Press, Cambridge, pp. 385–432.

Bird, M.I., Fitfield, L.K., Chua, S., Goh, B., 2004. Calculating sediment compaction for radiocarbon dating of intertidal sediments. *Radiocarbon* 46, 421–435.

Cahoon, D.R., Hensel, P., Rybczyk, J., McKee, K.L., Proffitt, C.E., Perez, B.C., 2003. Mass tree mortality leads to mangrove peat collapse at Bay Islands, Honduras after Hurricane Mitch. *Journal of Ecology* 91, 1093–1105.

Cahoon, D.R., Lynch, J.C., 1997. Vertical accretion and shallow subsidence in a mangrove forest of southwestern Florida, USA. *Mangroves and Salt Marshes* 1, 173–186.

Cameron, C.C., Palmer, C.A., 1995. The mangrove peat of the Tobacco Range Islands, Belize Barrier Reef, Central America. *Atoll Research Bulletin* 431, 1–32.

Chambers, F.M., Beilman, D.W., Yu, Z., 2011. Methods for determining peat humification and for quantifying peat bulk density, organic matter and carbon content for palaeostudies of climate and peatland carbon dynamics. *Mires and Peat* 7, 1–10.

Church, J.A., White, N.J., 2006. A 20th century acceleration in global sea-level rise. *Geophysical Research Letters* 33, L01602. http://dx.doi.org/10.1029/2005GL024826.

Cnudde, V., Boone, N.M., 2013. High-resolution X-ray computed tomography in geosciences: A review of the current technology and applications. *Earth Science Reviews* 123, 1–17.

Coates, A.G., McNeil, D.F., Aubry, M-P., Berggren, W.A., Collins, L.S., 2005. An introduction to the geology of the Bocas del Toro Archipelago, Panama. *Caribbean Journal of Science* 41, 374–391.

Davey, E., Wigand, C., Johnson, R., Sundberg, K., Morris, J., Roman, C.T., 2011. Use of computed tomography imaging for quantifying coarse roots, rhizomes, peat, and particle densities in marsh soils. *Ecological Applications* 21, 2156–2171.

Dean, W.E., 1974. Determination of carbonate and organic matter in calcareous sediments and sedimentary rocks by loss on ignition: comparison with other methods. *Journal of Sedimentary Petrology* 44, 242–248.

https://doi.org/10.1017/qua.2017.101 Published online by Cambridge University Press

Digerfeldt, G., Hendry, M.D., 1987. An 8000 year Holocene sea-level record from Jamaica: implications for interpretation of Caribbean reef and coastal history. *Coral Reefs* 5, 165–169.

Donnelly, J.P., Cleary, P., Newby, P., Ettinger, R., 2004. Coupling instrumental and geological records of sea-level change: evidence from southern New England of an increase in the rate of sea-level rise in the 19th century. *Geophysical Research Letters* 30, L05203. http://dx.doi.org/10.1029/2003GL017801.

Ellison, J.C., 1993. Mangrove retreat with rising sea-level, Bermuda. *Estuarine, Coastal and Shelf Science* 37, 75–87.

Ellison, J.C., Stoddart, D.R., 1991. Mangrove ecosystem collapse during predicted sea-level rise: Holocene analogues and implications. *Journal of Coastal Research* 7, 151–165.

Elyeznasni, N., Sellami, F., Pot, V., Benoit, P., Vieublé-Gonod, L., Young, I., Peth, S., 2012. Exploration of soil micromorphology to identify coarse-sized OM assemblages in X-ray CT images of undisturbed cultivated soil cores. *Geoderma* 179–180, 38–45.

Feller, I.C., McKee, K.L., Whigham, D.F., O'Neill, J.P., 2003. Nitrogen vs. phosphorus limitation across and ecotonal gradient in a mangrove forest. *Biogeochemistry* 62, 145–175.

Field, C.D., 1995. Impact of expected climate change on mangroves. *Hydrobiologia* 295, 75–81.

Gehrels, W.R., Kirby, J.R., Prokoph, A., Newnham, R.M., Achterberg, E.P., Evans, E.H., Black, S., Scott, D.B., 2005. Onset of recent rapid sea-level rise in the western Atlantic Ocean. *Quaternary Science Reviews* 24, 2083–2100.

Gehrels, W.R., Woodworth, P.L., 2013. When did modern rates of sea-level rise start? *Global and Planetary Change* 100, 263–277.

Gilman, E., Van Lavieren, H., Ellison, J., Jungblut, V., Wilson, L., Areki, F., Brighouse, G., et al., 2006. *Pacific Island Mangroves in a Changing Climate and Rising Sea*. United Nations Environment Programme Regional Seas Reports and Studies No. 179. United Nations Environment Programme, Regional Seas Programme, Nairobi, Kenya.

Gornitz, V, 1995. A comparison of differences between recent and late Holocene sea level trends from eastern North America and other selected regions. *Journal of Coastal Research* 1995, 287–297.

Green, M.A., Aller, R.C., Aller, J.Y., 1998. Influence of carbonate dissolution on survival of shell-bearing meiobenthos in nearshore sediments. *Limnology and Oceanography* 43, 18–28.

Hansson, S.V., Rydberg, J., Kylander, M., Gallagher, K., Bindler, R., 2013. Evaluating paleoproxies for peat decomposition and their relationship to peat geochemistry. *The Holocene* 23, 1666–1671.

Heijs, A.W.J., De Lange, J., Schoute, J.F.Th., Bouma, J, 1995. Computed tomography as a tool for non-destructive analysis of flow patterns in macroporous clay soils. *Geoderma* 64, 183–196.

Heiri, O., Lotter, A.F., Lemcke, G., 2001. Loss on ignition as a method for estimating organic and carbonate content in sediments: reproducibility and comparability of results. *Journal of Paleolimnology* 25, 101–110.

Helliwell, J.R., Sturrock, C.J., Grayling, K.M., Tracy, S.R., Flavel, R.J., Young, I.M., Whalley, W.R., Mooney, S.J., 2013. Applications of X-ray computed tomography for examining biophysical interactions and structural development in soil systems: a review. *European Journal of Soil Science* 64, 279–297.

Kaye, C.A., Barghoorn, E.S., 1964. Late Quaternary Sea-Level Change and Crustal Rise at Boston, Massachusetts, with Notes on the Autocompaction of Peat. *Geological Society of America Bulletin* 75, 63–80.

Ketcham, R.A., Carlson, W.D., 2001. Acquisition, optimization and interpretation of X-ray computed tomographic imagery: applications to the geosciences. *Computers and Geosciences* 27, 381–400.

Kettridge, N., Binley, A., 2011. Characterization of peat structure using X-ray computed tomography and its control on the ebullition of biogenic gas bubbles. *Journal of Geophysical Research* 116, G01024. http://dx.doi.org/ 10.1029/2010JG001478.

Khan, N.S., Ashe, E., Shaw, T.A., Vacchi, M., Walker, J.W., Peltier, W.R., Kopp, R.E., Horton, B.P., 2015. Holocene relative seal-level changes from near-, intermediate-, and far-field locations. *Current Climate Change Reports* 1, 247–262.

Kjerfve, B., Rützler, K., Kierspe, G.H., 1982. Tides at Carrie Bow Cay, Belize. In: Rützler, K., Macintyre, I.G. (Eds.), *The Atlantic Barrier Reef Ecosystem at Carrie Bow Cay, Belize. Smithsonian Contributions to the Marine Sciences* 12, 47–51.

Kolay, P.K., Shafiee, S.B., 2007. Hydraulic conductivity of tropical peat soil from Sarawak. EACEF – 1st International Conference of European Asian Civil Engineering Forum. Universitas Pelita Harapan, Jakarta, Indonesia, pp. A19–A25.

Koltes, K.H., Opishinksi, T.B., 2009. Patterns of water quality and movement in the vicinity of Carrie Bow Cay, Belize. In: Lang, M.A., Macintyre I.G., Rützler K. (Eds.), *Proceedings of the Smithsonian Marine Science Symposium. Smithsonian Contributions to the Marine Sciences* 38, 379–390.

Krauss, K.W., McKee, K.L., Lovelock, C.E., Cahoon, D.R., Saintilan, N., Reef, R., Chen, L., 2013. How mangrove forests adjust to rising sea level. *New Phytologist* 202, 19–34.

Kuhry, P., Vitt, D.H., 1996. Fossil carbon/nitrogen ratios as a measure of peat decomposition. *Ecology* 77, 271–275.

Lighty, R.G., Macintyre, I.G., Stuckenrath, R., 1982. *Acropora palmata* reef framework: a reliable indicator of sea-level in the western Atlantic for the past 10,000 years. *Coral Reefs* 1, 125–130.

Macintyre, I.G., Littler, M.M., Littler, D.S., 1995. Holocene history of Tobacco Range, Belize, Central America. *Atoll Research Bulletin* 430, 18.

Macintyre, I.G., Toscano, M.A., 2004. The Pleistocene foundation below Twin Cays, Belize, Central America. *Atoll Research Bulletin* 511, 1–17.

Macintyre, I.G., Toscano, M.A., Lighty, R.G., Bond, G., 2004. Holocene history of the mangrove islands of Twin Cays, Belize, Central America. *Atoll Research Bulletin* 510, 1–16.

Malmer, N., Holm, E., 1984. Variation in the C/N-quotient of peat in relation to decomposition rate and age determination with ^{210}Pb. *Oikos* 43, 171–182.

Mazda, Y., Kobashi, D., Okada, S., 2005. Tidal-scale hydrodynamics within mangrove swamps. *Wetlands Ecology and Management* 13, 647–655.

McKee, K.L., 2001. Root proliferation in decaying roots and old root channels: a nutrient conservation mechanism in oligotrophic mangrove forests? *Journal of Ecology* 89, 876–887.

McKee, K.L., 2011. Biophysical controls on accretion and elevation change in Caribbean mangrove ecosystems. *Estuarine, Coastal and Shelf Science* 91, 475–483.

McKee, K.L., Cahoon, D.R., Feller, I.C., 2007. Oceanic Islands keep pace with sea-level rise through feedback controls on mangrove root production. *Global Ecology and Biogeography* 16, 546–556.

McKee, K.L., Faulkner, P.L., 2000. Mangrove Peat Analysis and Reconstruction of Vegetation History at the Pelican Cays, Belize. *Atoll Research Bulletin* 468, 47–58.

McKee, K.L., Vervaeke, W.C., 2010. *Processing and Analysis of Wetland Peat Cores (I. Caribbean Mangrove Ecosystems)*. National Wetlands Research Center, Lafayette, Louisiana.

Middleton, B.A., McKee, K.L., 2001. Degradation of mangrove tissues and implications for peat formation in Belizean island forests. *Journal of Ecology* 89, 818–828.

Monacci, N.M., Meier-Grunhagen, U., Finney, B.P., Behling, H., Wooller, M.J., 2009. Mangrove ecosystem changes during the Holocene at Spanish Lookout Cay, Belize. *Palaeogeography, Palaeoclimatoligy, Palaeoecology* 280, 37–46.

Mooney, S.J., 2002. Three-dimensional visualization and quantification of soil macroporosity and water flow patterns using computed tomography. *Soil Use and Management* 18, 142–151.

Multer, H.G., Gischler, E., Lundberg, J., Simmons, K.R., Shinn, E.R., 2002. Key Largo Limestone revisited: Pleistocene shelf-edge facies, Florida Keys, USA. *Facies* 46, 229–271.

National Research Council, 2005. *The Geological Record of Ecological Dynamics: Understanding the Biotic Effects of Future Environmental Change*. Washington, DC: The National Academies Press. https://doi.org/10.17226/11209.

Nicholls, R.J., Wong, P.P., Burkett, V.R., Codignotto, J.O., Hay, J.E., McLean, R.F., Ragoonaden, S., Woodroffe, C.D., 2007. Coastal systems and low-lying areas. In: Parry, M.L., Canziani, O.F., Palutikof, J.P., van der Linden, P.J., Hanson, C.E. (Eds.), *Climate Change 2007: Impacts, Adaptation and Vulnerability. Contribution of Working Group II to the Fourth Assessment Report of the Intergovernmental Panel on Climate Change*. Cambridge University Press, Cambridge, pp. 315–356.

Ono, K., Fujimoto, K., Hiraide, M., Lihpai, S., Tabuchi, R., 2006. Aboveground litter production, accumulation, decomposition, and tidal transportation of coral reef-type mangrove forest on Pohnpei Island, Federated States of Micronesia. *Tropics* 15, 75–84.

Ono, K., Hirdate, S., Morita, S., Hiraide, M., Hirata, Y., Fujimoto, K., Tabuchi, R., Lihpai, S., 2015. Assessing the carbon compositions and sources of mangrove peat in a tropical mangrove forest on Pohnpei Island, Federated States of Micronesia. *Geoderma* 245–246, 11–20.

Page, S.E., Wust, R.A.J., Weiss, D., Rieley, J.O., Shotyk, W., Limin, S.H., 2004. A record of Late Pleistocene and Holocene carbon accumulation and climate change from an equatorial peat bog (Kalimantan, Indonesia): implications for past, present and future carbon dynamics. *Journal of Quaternary Science* 19, 625–635.

Parkinson, R.W., Delaune, R.D., White, J.R., 1994. Holocene sea-level rise and the fate of mangrove forests within the wider Caribbean region. *Journal of Coastal Research* 10, 1077–1086.

Paul, M.A., Barras, B.F., 1998. A geotechnical correction for post-depositional sediment compression: examples of the Forth Valley, Scotland. *Journal of Quaternary Science* 13, 171–176.

Perkins, R.D., 1977. Depositional Framework of Pleistocene rocks in south Florida. In: Enos, P., Perkins, R.D. (Eds.), Quaternary Sedimentation in South Florida. GSA Memoir Vol. 147. Geological Society of America, Denver, Colorado. pp. 131–198.

Pierret, A., Capowiez, Y., Belzunces, L., Moran, C.J., 2002. 3D reconstruction and quantification of macropores using X-ray computed tomography and image analysis. *Geoderma* 106, 247–271.

Pizzuto, J.E., Schwendt, A.E., 1997. Mathematical modeling of autocompaction of a transgressive valley fill deposit, Wolfe Glade, Delaware. *Geology* 25, 57–60.

Quinton, W.L, Elliot, T., Price, J.S., Rezanezhad, F., Heck, R., 2009. Measuring physical and hydraulic properties of peat from X-ray tomography. *Geoderma* 153, 269–277.

Rezanezhad, F., Quinton, W.L., Price, J.S., Elrick, D., Elliot, T.R., Heck, R.J., 2009. Examining the effects of pore size distribution and shape on flow through unsaturated peat using computed tomography. *Hydrology and Earth System Science* 13, 1993–2002.

Robbin, D.M., 1984. A new Holocene sea-level curve for the upper Florida Keys and Florida reef tract. In: Gleason, P.J. (Ed.), *Environments of South Florida, Present and Past*. Miami Geological Society, Miami, Florida, pp. 437–458.

Scholander, P.F, van Dam, L., Scholander, S.I., 1955. Gas exchange in the roots of mangroves. *American Journal of Botany* 42, 92–98.

Shaw, J., Ceman, J., 1999. Salt-marsh aggradation in response to late-Holocene sea-level rise at Amherst Point, Nova Scotia, Canada. *The Holocene* 9, 439–451.

Shennan, I., Lambeck, K., Horton, B.P., Innes, J., Lloyd, J., McArthur, J., Rutherford, M., 2000. Holocene isostasy and relative sea-level on the east England coast. In: Shennan, I., Andrews, J. (Eds.), *Holocene Land-Ocean Interaction and Environmental Change around the North Sea. Geological Society Special Publications* Vol. 166. Geological Society of London, London, pp. 275–298.

Skelton, N. J, Allaway, W.G., 1996. Oxygen and pressure changes measured in situ during flooding in roots of the Grey Mangrove *Avicennia marina* (Forssk.) Vierh. *Aquatic Botany* 54, 165–175.

Sleutel, S., Cnudde, V., Masschaele, B., Vlassenbroek, J., Dierick, M., Van Hoorebeke, L., Jacobs, P., De Nevea, S., 2008. Comparison of different nano- and micro-focus X-ray computed tomography set-ups for the visualization of the soil microstructure and soil organic matter. *Computers and Geosciences* 34, 931–938.

Srikanth, S., Kaihekulani, S., Lum, Y., Chen, Z., 2016. Mangrove root: adaptations and ecological importance. *Trees* 30, 451–465.

Stanley, S.M., 1966. Paleoecology and diagenesis of the Key Largo Limestone, Florida. *American Association of Petroleum Geologists Bulletin* 50, 1927–1947.

Stumpf, R.P., Haines, J.W., 1998. Variations in tidal level in the Gulf of Mexico and implications for tidal wetlands. *Estuarine, Coastal and Shelf Science* 46, 165–173.

Taina, I.A., Heck, R.J., Elliot, T.R., 2008. Application of X-ray computed tomography to soil science: a literature review. *Canadian Journal of Soil Science* 88, 1–19.

Tanaka, A., Nakano, T., 2009. Data report: three-dimensional observation and quantification of internal structure of sediment core from Challenger Mound area in Porcupine Seabight off western Ireland using a medical X-ray CT. *Proceedings of the Integrated Ocean Drilling Program* 307, 1–24.

Törnqvist, T.E., Van Ree, M.H.M., Van't Veer, R., Van Geel, B., 1998. Improving methodology for high-resolution reconstruction of sea-level rise and neotectonics by paleoecological analysis and AMS ^{14}C dating of basal peats. *Quaternary Research* 49, 72–85.

Törnqvist, T.E., Wallace, D.J., Storms, J.E.A., Wallinga, J., Dam, R.L., Blaauw, M., Derksen, M.S., Klerks, C.J.W., Meijneken, C., Snijders, E.M.A., 2008. Mississippi Delta subsidence primarily caused by compaction of Holocene strata. *Nature Geoscience* 1, 173–176.

Toscano, M.A., Lundberg, J., 1998. Early Holocene sea-level record from submerged fossil reefs on the southeast Florida margin. *Geology* 26, 255–258.

Toscano, M.A., Macintyre, I.G., 2003. Corrected western Atlantic sea-level curve for the last 11,000 years based on calibrated ^{14}C dates from *Acropora palmata* framework and intertidal mangrove peat. *Coral Reefs* 22, 257–270.

Urish, D.W., Wright, R.M., Rodriguez, W., Feller, I.C., 2009. Dynamic hydrology of a mangrove island: Twin Cays, Belize. In: Lang, M.A., Macintyre, I.G., Rützler, K. (Eds.), *Proceedings, Smithsonian Marine Science Symposium* (Smithsonian Contributions to the Marine Sciences 38. Smithsonian Institution, Washington, DC, pp. 473–490.

US Federal Geographic Data Committee, Marine and Coastal Spatial Data Subcommittee, 2012. Coastal and Marine Ecological Classification Standard (CMECS). Document number FGDC-STD-018-2012. Available at https://www.fgdc.gov/standards/projects/FGDC-standards-projects/cmecs-folder/cmecs-index-page (accessed).

Whelan, K.R.T., Smith, T.J. III, Cahoon, D.R., Lynch, J.C., Anderson, G.H., 2005. Groundwater control of mangrove surface elevation: shrink and swell varies with soil depth. *Estuaries* 28, 833–843.

Williams, H.F.L., 2003. Modeling shallow autocompaction in coastal marshes using Cesium-137 fallout: Preliminary results from the Trinity River Estuary, Texas. *Journal of Coastal Research* 19, 180–188.

Woodroffe, C.D., 1990. The Impact of sea-level rise on mangrove shorelines. *Progress in Physical Geography* 14, 483–520.

Woodroffe, C.D., 1995. *Mangrove Vegetation of Tobacco Range and Nearby Mangrove Ranges, Central Belize Barrier Reef* (Atoll Research Bulletin, No. 427. Museum of Natural History, Smithsonian Institution, Washington, DC.

Wooller, M.J., Morgan, R., Fowell, S., Behling, H., Fogel, M., 2007. A multiproxy peat record of Holocene mangrove paleoecology from Twin Cays, Belize. *The Holocene* 17: 1129–1139.

Yu, Z., Campbell, I.D., Campbell, C., Vitt, D.H., Bond, G.C., Apps, M.J., 2003. Carbon sequestration in western Canadian peat highly sensitive to Holocene wet-dry climate cycles at millennial timescales. *The Holocene* 13, 801–808.

https://doi.org/10.1017/qua.2017.101 Published online by Cambridge University Press